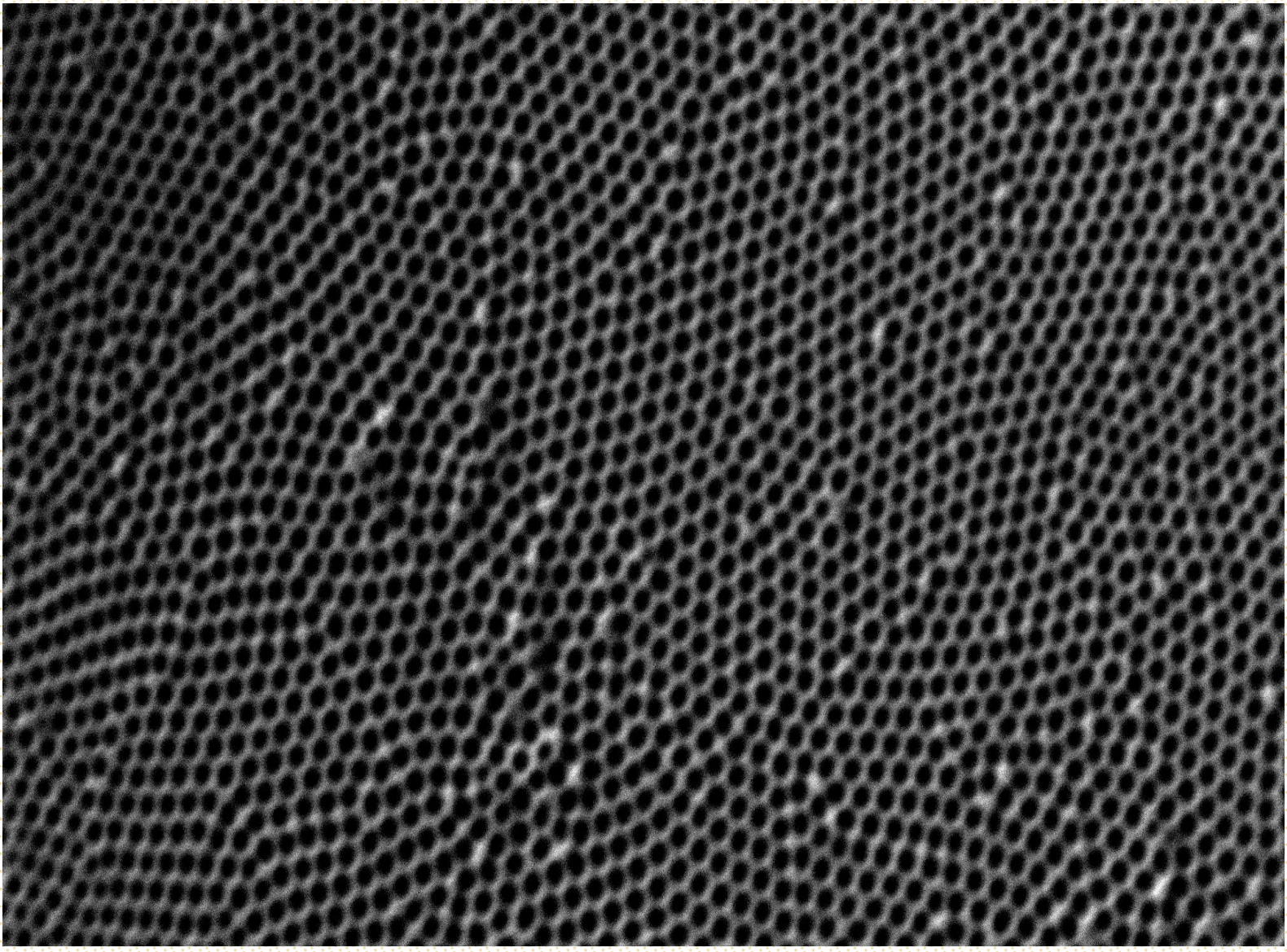

Ayesha Khalid

Tribological Behavior of Micro/Nano Structured Tantalum Surfaces by Anodization Method

Submitted in partial fulfillment of the requirements for the degree of Master in Tribology of Surface and Interfaces

July 2016

· U C ·

UNIVERSIDADE DE COIMBRA

FCTUC FACULDADE DE CIÊNCIAS
E TECNOLOGIA
UNIVERSIDADE DE COIMBRA

DEPARTAMENTO DE
ENGENHARIA MECÂNICA

Tribological Behavior of Micro/Nano Structured Tantalum Surfaces by Anodization Method

Submitted in Partial Fulfilment of the Requirements for the Joint European Master in Tribology of Surfaces and Interfaces

Author

Ayesha Khalid

Advisors

Professor Amilcar Ramalho
Professor Sandra Carvalho

Jury

President	**Bruno Trindade** **Professor at University of Coimbra**
Vowels	**Paulo Ferreira** **Professor at University of Texas** **Stephen Muhl** **Professor at National Autonomous University of Mexico**
Advisor	**Amilcar Ramalho** **Professor at University of Coimbra**

In the framework of Joint European Master in Tribology of Surfaces and Interfaces

tribos Joint European Master in Tribology of Surfaces and Interfaces
Ljubljana • Leeds • Coimbra • Luleå

Coimbra, July, 2016

"When I'm working on a problem, I never think about beauty. I think only how to solve the problem. But when I have finished, if the solution is not beautiful, I know it is wrong."

(R. Buckminster Fuller)

ACKNOWLEDGEMENTS

As I come to the end of my thesis and put the final touch of acknowledging all the people who helped and supported me through this I reflect back to this period of intense learning, not just on academic level but also on a personal level.

I would first and foremost like to express my profound gratitude to my supervisors Professor Sandra Carvalho and Professor Amilcar Ramalho who were always available whenever I needed guidance. I am grateful to Professor Albano for his help, patience and support and for facilitating me in every way possible. I am especially thankful to Professor Amilcar for his valuable guidance and for inspiring me to think out of the box in scientific research. I am also thankful to Cristiana Alves for her support and guidance. She was a valuable mentor on my visits University of Minho for experimental work.

I am thankful to the TRIBOS consortium for providing me with the opportunity of pursuing my master studies under this prestigious program. A special thanks to all my TRIBOS mentors Professor Ardian Morina, Professor Mitjan Kalin and Professor Bruno Trindade for their support.

Lastly, I would like to acknowledge the iron support of my family, especially my mother and my fiancé, through this journey. I thank you for being my cheerleaders in hard times and pushing me to do my best.

ABSTRACT

Tantalum is a metal which has shown to have excellent biocompatibility and bioactivity, making it a potential material for dental implant. Nano texturing can improve the performance of Ta dental implant as it promotes faster osseointegration. Nano texturing changes surface roughness which affects the tribological behavior.

An electrochemical process called anodization was used to modify the surface of tantalum by introducing highly ordered nano pores on its surface. Anodization is a process that involves several parameters which can be easily modified to produce controlled surface texturing. The applied potential has a propotional relationship to pore diameter and Ta_2O_5 film thickness. Higher applied potential leads to larger pore diameters and thicker oxide layer. For the purpose of this thesis, tantalum was anodized at three different potentials, namely 15, 25 and 50 V. The purpose of this thesis was to test the effect of surface roughness induced by anodization, on the tribological properties of Ta, particularly its static friction behavior. The surface roughness parameter used for this study was the mean peak to valley height of profile (Rz). Reference samples used for comparison were polished Ta metal and chemically etched Ta.

Structural analysis of the prepared Ta samples was performed by optical microscopy, surface morphology was characterized by scanning electron microscopy (SEM), the crystal structure was examined by X-ray diffraction (XRD), hardness was measured using Vickers hardness method and surface roughness measurements were made by a 3-D profilometer. Friction tests were performed using a standard tensile testing machine with electronic control of cross head motion.

Highly ordered nano porous surface was formed by the anodization process. The size of pores increased when higher anodization potentials were used. The anodization process caused a change in surface roughness. The relationship between surface roughness and the static friction coefficient was studied and it was found that static friction coefficient showed a propotional relationship to surface roughness. Dynamic friction coefficient did not show a clear relation to surface roughness.

] **keywords**: Tantalum, anodization, nano-texturing, surface roughness, tribology, static friction.

RESUMO

O Tântalo (Ta) é um elemento metálico com excelentes propriedades no que diz respeito a biocompatibilidade e bioatividade, demonstrando possuir um enorme potencial para ser usado em implantes odontológicos. A nano-texturização pode melhorar o desempenho de implantes dentários promovendo um aumento por parte da integração óssea. No entanto, a alteração da rugosidade superficial através desta técnica de superfície pode afetar o seu comportamento tribológico. No presente trabalho, foi utilizado um processo eletroquímico conhecido como anodização de forma a modificar a superfície do Ta através da introdução de nano poros, altamente ordenados. A anodização é um processo que envolve a utilização de vários parâmetros que podem ser facilmente modificados, permitindo obter um maior controle sobre a texturização da superfície do elemento. Existe uma relação diretamente proporcional entre o potencial aplicado (Volts-V) e o diâmetro dos poros assim como a espessura dos filmes de Ta_2O_5. Quanto maior for o potencial aplicado, maior será o diâmetro dos poros e mais espessa será a camada de óxido formada sobre a superfície de Ta.

O presente trabalho tem como objetivo o estudo do efeito da alteração da rugosidade na superfície de Ta induzida por anodização, assim como, a influência sobre as propriedades tribológicas, em particular o seu comportamento à fricção estática. Para que este estudo fosse possível foi realizada a análise estrutural e morfológica de amostras anodizadas a três potenciais diferentes: 15, 25 e 50 V.

A análise estrutural das amostras de Ta foi avaliada com recurso à técnica de difração de raios-X (DRX), a morfologia da superfície foi estudada por microscopia de varrimento eletrónico (SEM), a dureza classificada segundo a escala de Vickers e a rugosidade avaliada através de um perfilómetro 3-D. Os ensaios de desgaste foram realizados utilizando uma máquina de ensaios de tração com controlo numérico. Os resultados obtidos foram comparados com amostras de Ta sem qualquer tratamento superficial.

O processo de anodização permitiu obter superfícies nano porosas extremamente ordenadas. O tamanho das porosidades aumentou com o aumento do potencial de anodização. A utilização do processo de anodização possibilitou uma alteração da rugosidade superficial. A relação entre a rugosidade superficial e o coeficiente de atrito estático, foi comparada, verificando-se que o valor de coeficiente de atrito é

diretamente proporcional á rugosidade superficial. Em relação ao coeficiente de atrito dinâmico, não foi encontrado uma relação empírica com a rugosidade superficial.

palavras-chave: Tântalo, anodização, nano-texturização, rugosidade superficial, tribologia , atrito estático .

Contents

LIST OF FIGURES

LIST OF TABLES

SYMBOLOGY AND ACRONYMS

Symbology

μ_s – static friction coefficient
μ_d – dynamic friction coefficient

Acronyms

ICDD – International centre for diffraction data

CEMUC – Centre for Mechanical Engineering

HV – Vickers hardness

1. INTRODUCTION

A dental implant is an artificially constructed tooth root which is integrated with an artificially made tooth crown to replace missing teeth [1]. When the implant is inserted inside the jaw, a healing process takes place. The healing process is called osseointegration, which occurs when the bone cells surround the implant grow into a network around the artificial prosthetic, hence holding it firmly in place. The growing bone cells are called osteoblasts. Their adhesion to the implant surface greatly depends on the implant geometry and surface properties. Biocomplatibility is the most essential property required for dental implant materials. In this regards tantalum seems to be a good option.

Modification of surface properties of a dental implant has been given special focus in terms of accelerating the healing process. Particularly surface roughness has been identified as an important parameter in this respect [2]. Several surface texturing techniques have been used in the past but each of them has certain drawbacks. Most importantly, the techniques do not provide easy control of surface roughness. Anodization is an electrochemical technique that has been employed in the past for surface texturing. The parameters involved in this technique can be easily controlled, hence giving the user to ability to control the surface roughness. The technique can be used to achieve surface roughness values from the micron scale down to the nano scale.

The tribological behavior of a textured dental implant surface plays a significant role in its performance. When a dental implant is inserted inside the jaw, ideally it should become anchored firmly with no motion. The efficiency of mechanical interlocking between the textured surface and the surrounding bone decides the degree of the anchorage. The mechanical interlocking also decides how much force would be required to slide the contacting surfaces against each other. In a dental implant sliding should not exist. Therefore, the textured surface should have a surface roughness that enables it to efficiently interlock with the bone structure. In other words, its static friction coefficient should be as high as possible. However, dental implants have shown to exhibit some fretting motion. Fretting can lead to wear debris and loosely anchored dental implant. Therefore it is essential to study the tribological behavior of the material used for dental implant in order to validate its suitability for the application.

The purpose of this master's thesis is to study the tribological behavior of micro/nano anodized tantalum surface by anodization to be used as dental implant

materials. Tantalum surfaces with different nano pore sizes have been made by anodization and the tribological performance of these surfaces in contact with bone will be evaluated.

1.1. Objectives

The aim of this master thesis research work is to measure and analyze the tribological behavior of micro/nano textured tantalum surfaces formed by anodization method. Anodization is an electrochemical technique that has been employed in the past for surface texturing of materials for different applications. For dental implants, surface texturing has been performed to accelerate the healing process. The anodization technique involves several parameters which can be easily controlled to modify the surface texture and to achieve highly ordered nanopores. For this thesis, the applied potential was varied while keeping all other parameters (time, electrolyte, current and temperature) constant. Increasing the potential causes the pore diameter and the tantalum oxide layer thickness to increase.

Surface morphology was characterized by scanning electron microscope (SEM), the crystal structure by X-ray diffraction (XRD), the surface roughness by 3-D profilometry and hardness by vickers hardness test. The tribological characterization was done by using a friction coefficient measurement device which was originally developed in CEMUC. The setup was operated by a standard tensile testing machine where the cross head motion was controlled electronically. The wear marks were analyzed under an optical microscope. The friction tests were performed at both dry and wet conditions. For the wet conditions, the ageing effect of saliva was studied by immersing the samples in aritificial saliva for 3 days, after which, friction tests were performed.

1.2. Thesis Structure

This thesis titled “Tribological properties of micro/nano textured tantalum surfaces by anodization method” was performed as partial requirement for the completion of masters in tribology of surfaces and interface (TRIBOS).

The thesis is divided into five parts. Chapter 1 describes the objectives and structure of the thesis. The state of the art is presented in Chapter 2. The experimental methods and the materials used as well as the characterization techniques are explained in

Chapter 3. The results and discussion are presented in Chapter 4. The conclusions are given in Chapter 5 and the future work is presented in Chapter 6.

2. STATE OF THE ART

2.1. Dental Implants

Tantalum is a high density, high strength and high hardness metal. It has been studied in the past for its possible biomedical applications and it has shown to have good biocompatibility and bioactivity [1], [2]. The factors that contribute to the high bioactivity in tantalum are its higher surface wettability and surface energy as compared to titanium which lacks bioactivity [25], therefore tantalum has potential application as dental implant.

A dental implant is an artificially constructed tooth root which is integrated with artificially made tooth crown to replace missing teeth [1]. A dental implant is designed to match as closely as possible to the real tooth root. A comparison of natural tooth and a dental implant is given in Figure 2.1.

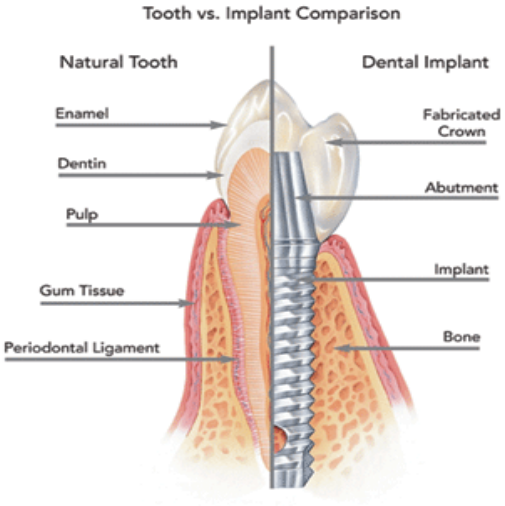

Figure 2.1. Tooth vs. Implant Comparison [**5]**

In this figure the different components of artificial tooth are given. The implant is in direct contact with the surrounding bone. When the implant is inserted inside the jaw, a healing process takes place. The healing process is called osseointegration. The concept of osseointegration was first introduced by Brånemark [3]. In his research paper he concluded that the typical healing time for a dental implant is 3 to 6 months. Since the advent of dental implants in 1965 [4], various methods of improving the performance of the artificial prosthetic have been researched. Osseointegration occurs when the bone cells

surround the implant grow into a network around the artificial prosthetic, hence holding it firmly in place. The growing bone cells are called osteoblasts. Their adhesion to the implant surface greatly depends on the implant geometry and surface properties. Titanium is a popular material used to make dental implant due to its excellent corrosion resistance, high strength and excellent biocomplatibility. Titanium forms an oxide upon exposure to air. The oxide layer is biocompatible and bioinert . Hence bone cells are not easily bonded with its surface, resulting in the formation of a fibrous tissue layer which subsequently separates the metal surface from the cells. Tantalum is another biocompatible material which forms a bioactive oxide layer on its surface and thus has exhibited a behavior much closer to real bone behavior than titanium [25]. Therefore this research has focused on tantalum as a dental implant material because tantalum holds the promise of a faster and more effective healing process.

2.2. Surface modification of dental implant

Modification of surface properties has been given special focus in terms of improved biocompatibility of dental implant material. Particularly surface roughness has been identified as an important parameter in the acceleration of healing process [2]. A research study was conducted by Albrektsson & Wennerberg [7] on the effect of surface roughness on dental implant performance. They focused their research on four most commonly used commercially available dental implants. They categorized dental implants according to their surface roughness values as: smooth (Sa < 0.5 µm), minimally rough (Sa = 0.5-1.0 µm), moderately rough (Sa = 1.0-2.0 µm) and rough (Sa > 2.0 µm) [2]. The researchers also introduced a new surface roughness parameter, developed surface area ratio (Sdr) which takes into account the density of peaks (Sds) and surface roughness (Sa). Hence it is a hybrid parameter used to estimate the heights and peaks of a surface [2]. Surface roughness can be divided into three levels based on scale [8]: macro, micro and nano scaled roughness.

Several surface modification techniques have been used in the past. The most commonly used surface modification techniques are: sand blasting (mechanical method), acid etching (chemical method), plasma spraying (coating method), laser modification and anodization (electrochemical method) [8].

Sand blasting is a process by which the surface is impinged by particles, creating grooves and craters. This way the surface roughness is increased. Wennerberg et.

al. performed extensive research on this method of surface modification on commercially pure titanium implants [9][10]. They were able to conclude that the surface roughness depends on the size, speed, density and shape of the impinging particle. The impinging particles used were titanium oxide and aluminum oxide. A drawback of sand blasting is that sometimes the particles can become buried in the surface. Typical surface roughness values obtained from this method are 0.5 – 2.0 µm [2].

Acid etching is a technique by which an acid is used to pit the surface, selectively removing some grains and grain boundaries. A surface can be made of different phases. Compositional differences result in different sensitivity to acid etching. Hence, some phases are more easily removed than others, resulting in increased surface roughness by pitting. The surface roughness depends on the type of acid used, soaking time and material surface composition. Typical surface roughness values obtained from acid etching are 0.3 – 1.0 µm [2].

Coating methods such as plasma spraying have been used in the past as well. Groot et. al. researched the possibility of improving the biocompatibility of titanium implants by coating the surface with hydroxyapatite [11]. Their reason for using this particular coating is its close match with bone. Past research has shown that the coating effectively increases osseointegration, However, the coatings have weak adhesion on the metal surface. They can dissolve when the implant is inserted or develop long term failure [12].

2.2.1. Anodization

Bone cells (osteoblasts) have been shown to exhibit greater adhesion to nano-textured titanium than to conventional titanium [12]-[14]. Hence, nanotexturing has shown to improve the osseointegration process. Anodization is an electrochemical technique that has been employed in the past for surface texturing of materials for different applications. In the medical sector, anodization has been used to modify the surface properties of implants. The anodization process consists of three major steps as given in literature [12]: alkaline cleaning, acid activation and electrolyte anodizing. The anodization is an electrochemical process which is carried out in a typical three electrode cell: Sample anode, platinum cathode and Ag/AgCl reference electrode. The two electrode cell can also be used. The technique can be used in two modes: constant potential and constant current. Anodization has been used for inducing micro and nanopores on tantalum oxide surface, in

past research. The electrochemical reactions and ions diffusion that take places during the process lead to the formation of an oxide on the anode.

The earliest studies on anodization involved high voltage anodization (ASD). The mechanism behind surface texturing by this method can be explained by the avalanche theory [12]. When an oxide film forms it acts as a dielectric barrier to current flow. As the potential is increase, the film continues to grow until the dielectric breakdown limit is reached. At this point, the weaker regions of the heterogenous oxide film undergo thermal stressing and subsequent breakdown. The exposed metal below the oxide starts forming an oxide layer again. Therefore the process involves a balance between the growth and breakdown of the oxide film. The balance is dependent on the processing parameters given above, especially the type of electrolyte chosen for the technique plays a major role. Figure 2.2 shows the anodization process:

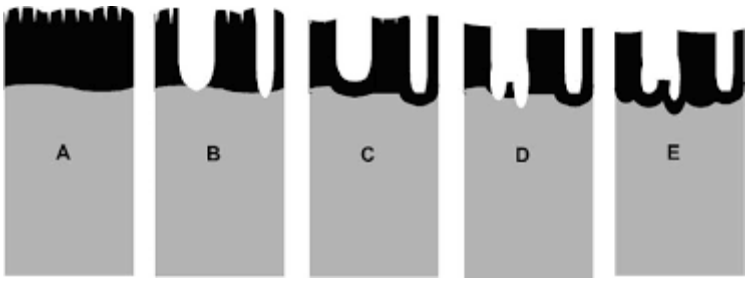

Figure 2.2. Schematic diagram of porous titanium oxide formation above the breakdown potential: (A) oxide growth to maximal thickness (B) burst of oxide by the formation of crystallites (pore formation), (C) immediate repassivation of pore tips, (D) burst of repassivated oxide, and (E) dissolution of the formed oxide and second repassivation [16].

There are several parameters that control the anodization process [12]:

electrolyte composition & concentration

- Potential
- Current
- pH (type of acid used)
- temperature
- time

The effect of different types of electrolytes on oxide growth has been studied in the past by Sul et. al.[15]. They conducted their studies on the most commonly used electrolytes for anodization: sodium oxide, sulphuric acid, phosphoric acid,acetic acid and calcium hydroxide. They observed that acidic electrolytes produced thicker films than

alkaline electrolytes. A number of researchers have studied the formation of TiO_2 nanotubes on oxide thin film by anodization.

In 1980, Baun was able to form nanoporous TiO_2 by anodization in chromic acid at 10-40 V [17]. Since then, a number of researchers have found that presence of hydrogen fluoride (HF) in electrolyte leads to formation of nanoporous structures TiO_2 at relatively lower voltages [18]-[22].

The effect of using different potential values in HF solution was studied by Gong et. al. [[23]] and they found that as potential is increased, the pore size increases but the final length of the nanotubes was independent of pore size [23].

The pH of the electrolyte bath affects the ability of oxide to reform after breaking and the ability of electrolyte to dissolve the oxide [24]. Cai et. al. [25] studied the effect of electrolyte pH on the growth of nanotubes on titanium oxide surface. They observed that increasing the pH increases the time required for nanotube formation. Longer nanotubes could be obtained at higher pH [25]. Hence the nanotube length can be controlled by controlling the pH. The anodization time influences the nanotube wall thickness but does not affect the tube diameter. With an increase in time the tube wall thickness increases [24].

The pore wall thickness can be varied by changing the electrolyte bath temperature. This relationship was studied by Mor GK et. al. [26]. They found out that varying the temperature varied the process of electrochemical etching and chemical dissolution. They performed their experiments at a constant potential of 10 V and two different temperatures: 5 ˚C and 50 ˚C. The pore diameter is both cases was the same but the average pore wall thickness at 5 ˚C was 34 nm and at 50 ˚C it was 9 nm.

Biological studies have shown a high healing rate in anodized nanoporous TiO_2 dental implant. This is due to the increased adhesion, attachment and growth of the osteoblasts on the bone-mimicking nanoporous surface. The osteoblasts have also shown to have a different morphology on anodized surface than on unanodized titanium. They show greater spreading on the surface of anodized titanium whereas they appear more rounded on unanodized titanium [13]. The nanotubular structure also promoted much higher calcium deposition by osteoblasts than the low roughness surface.

In the extensive study and research on the application of titanium as a biocompatible material, it has been discovered that even though titanium oxide has excellent biocompatibility, it lacks sufficient osseointegration for implant longetivity [27].

As discussed in chapter 2.2, surface modification of dental implant, different surface texturing methods have been used to promote bioactivity in titanium surface by improving its adhesion and mechanically interlocking with bioactive coatings. Titanium oxide surfaces need to be coated with a more bioactive hydroxyapatite to improve their osseointegration performance. But ceramic porous coatings carry the risks of delamination, cracking and low fracture toughness [27]. A bioactive material should not require any coatings; its own surface should encourage bone growth [28]. Tantalum has come into the spotlight as a material with good bioactivity, high mechanical strength and excellent fatigue resistance [28]. The only reason its application in the medical field has been limited is the processing problems associated with the metal. Tantalum is an expensive material with a high melting point and high affinity to oxygen. This has posed as an obstacle in manufacturing of a fully dense tantalum implant. In 2010, Balla et. al. [27] performed laser coating of tantalum on titanium for bone replacement structures. Their study found that Ta coated implant showed enhanced cell attachment and proliferation as compared to titanium oxide surface. The enhanced osseointegration was attributed to the superior wettability and high surface energy of Ta surface [27]. Jafari et. al. [29] compared the performance of porous tantalum hip cup and hydroxyapatite coated titanium hip cup. Their aim was the compare the bioactivity of both materials. Ta hip cup exhibited superior performance than HA coated Ti cup. They concluded that Ta has clear potential for bone ingrowth whereas Ti surface has potential for bone ongrowths. It requires an assistive bioactive coating such as HA, hence it is not a true bone ingrowth surface (lacks bioactivity) [29].

The anodization of tantalum oxide films, both amorphous and crystalline has been given special focus. The growth of dense oxide on tantalum in dilute phosphoric acid electrolyte was studied by Lu et. al. in 2002 [30]. The growth of porous Ta_2O_5 films in mixed H_2SO_4/HF electrolyte was studied by Sieber et. al. [31]. It was found that the nearly uniform porous oxide can be achieved with pore diameter ranging from 2 to 10 nm. The morphology and thickness of the layer depends on applied potential, anodization time and the concentration of HF [31]. Anodization of tantalum has also been performed in non-aqueous electrolytes consisting of glycerol with small quantities of NH_4 [32]. It was found that porous layers of thickness up to 15 µm and pore diameters in the range of 10-40 nm can be achieved by optimizing the electrochemical conditions [32]. This study also confirmed the strong effect of fluoride concentration and applied potential on the morphology of the layers. Allama et. al. [33] studied the effect of using different concentrations of HF and H_2SO_4. In addition they also studied the effect of adding small

amounts of different additives such as H_3PO_4, ethylene glycol and dimethyl sulfoxide. They observed that pore diameter increases with increasing concentration of HF. Addition of H_3PO_4 resulted in growth of higher lengths of nanorods (1300 nm) and the other additives enabled fabrication of high aspect-ratio vertically oriented tantalum oxide nanotube array films [33].

Hence the same principals of controlling anodization parameters for texturing titanium can also be applied for tantalum oxide surface, making its processing an economical and simple task.

Anodic oxidation of tantalum can be used to produce controlled surface porosity at the micro and nano scale. It has proven to be a simple, efficient technique for surface texturing of dental implants. Anodized surfaces have shown to have higher biocompatibility and lead to better adhesion and network formation from osteoblasts. Since tantalum has excellent biocompatibility, its nanoporous oxide surface can potentially lead to shorter healing time.

2.3. Dental implant/Bone interface: Tribological Problems

The design of a dental implant may be improved and optimized to match as closely as possible to the real tooth but there will still be some differences. The mechanical interlocking between a dental implant surface and the surrounding bone is not as strong as the real biological surfaces of tooth and bone.

In chapter 2.2 the importance of surface texturing was discussed. Texturing of the implant surface is performed to provide it with a surface structure that will fit into the nano-porous structure of the bone. The two surfaces can ideally be thought of as having complimenting jigsaw pattern, although the mechanical interlocking would not be as perfect as a jigsaw. This interlocking provides the initial mechanical anchorage to the implant/bone interface while the bone grows around the implant. Friction plays a major role in the initial stability of immediately loaded dental implants [34]. It results from the mechanical interlocking of implant and bone surfaces. Good mechanical interlocking means that under loaded conditions the interface should undergo minor elastic deformations but no slippage, as slippage will lead to micro-motions which result in problems as will be explained further. Keeping this mechanical interlocking phenomenon in mind, researchers have been improving the surface properties of dental implants. In

1972, Predcki et. al. studied the effect of threaded implants as compared to smooth implants, on the attachment of bone [35]. They found that the threaded implants showed greater bone growth due to better mechanical interlocking and osseointegration. Researchers also developed porous coatings in order to improve friction properties of the implant [36]. The idea was that the increased surface roughness will improve implant fixation. But studies have found that only a small percentage of pore volume is actually filled with bone [37]-[39]. In 2012, Hasan et. al. researched an experimental approach to determine the friction coefficient of implant-antler interface [34]. The antler is similar in nature to human bone; hence the static and kinetic friction coefficients were measured. The static friction coefficient values came to be in the range of 0.5-0.7 and increasing sliding velocity decreased the friction coefficient [34]. A finite element method was also developed by Bulaqi et. al [40] to study the effect of coefficient of friction on the preload induced at the implant/bone interface and other interfaces of implant system. They were able to conclude that coefficient of friction plays the most important role in implant screw loosening [40].

In reality the implant's surface does not interlock with the bone surface quite as efficiently as desired. This causes some micro-motion to occur between the implant and bone and the knowledge of the implications of this micro-motion on the performance of the dental implant is important. tribological implications. The following paragraphs explain the state of the art of the micro-motion problems that exist in dental implants.

In the earliest studies on the application of titanium dental implants, the existence of some small degree of motion between the implant and bone was pointed out by Carlsson et. al.[41]. This small degree of motion is called fretting. Fretting is the tribological motion between two contacting surfaces under loaded condition, where the amplitude of the movement is less than 100 μm [42]. The dental implant/bone interface undergoes fretting wear due to the chewing motion of the mouth. The motion turns the dental implant/bone interface into a special tribological pair undergoing different stresses (tension, compression, shear) resulting in complex fretting and ultimately failure [1]. It is especially a prominent problem during the early stages of osseointegration. After insertion of the dental implant, the healing process takes a few months. In the primary healing phase the fretting motion is highest as the surrounding bone has not fully attached itself to the implant. The fretting behavior of titanium implants/cortical bone interface was studied by Yu et. al. in 2005 [43].

In a bio-tribological system, fretting will not just lead to production of wear debris and surface damage. One of the contacting surfaces is the bone which is a living tissue. It grows with time around the implant. The bio-response of the bone and the process of osseointegration are also affected due to fretting motion. Fretting in dental implant/bone interface can be divided into three types which are also illustrated in Figure 2.3 [44]:

1. tangential fretting
2. radial fretting
3. dual-motion fretting

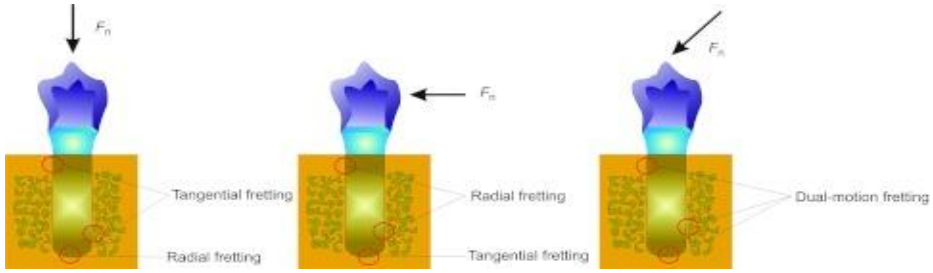

Figure 2.3. Fretting modes existed in the dental implant/bone interface [44]

Yu et. al. in their research on fretting of titanium implants as mentioned before, studied the tagential mode of fretting. They performed their experiments in-vitro by employing a titanium ball on bone flat geometry on a reciprocating tribometer modified for fretting. They were able to conclude that tagential fretting occurs due to delamination and abrasive wear [43].

In 2008, Yu HY et. al. studied the radial fretting behavior of cortical bone/ titanium implant interface [45]. Radial fretting behaves quite differently from tagential fretting due to the different direction of loading. The researchers concluded from their study that radial fretting results in four types of cracks. The most common were along the cement line due to the deficiency of calcium and phosphate along those lines. ‘The second cracks initiate from or end at the Havers's canal. The third ones are cracks connecting two consecutive Havers's canals if the stress is big enough. Each Harvers's system is a relative independent structure, but it will release the stress energy to adjacent Harvers's system if it could not use out the high stress brought from cracks alone. The fourth type is that kind of cracks propagating at interstitial lamella linearly’ [45]. The four types of cracks are given in Figure 2.4 [44]:

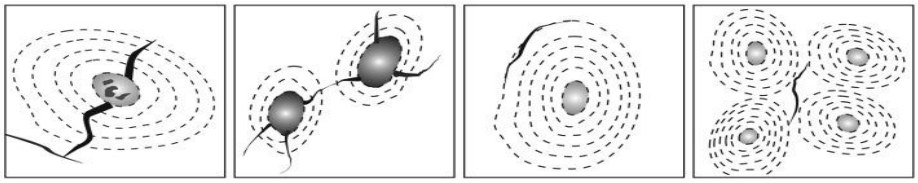

Figure 2.4. Four kind of cracks in radial fretting test [44].

Since the implant/bone interface is loaded under different forms of stresses due to the masticatory movement, fretting at the interface cannot so simply be defined as purely tangential or radial. In fact, dual motion fretting occurs more commonly than either of the latter two. Keeping this in mind, Yu HY et. al. expanded their research in 2009 and studied the dual motion fretting behavior of titanium implant/bone interface [46]. They found that at low loads, the main wear mechanisms of dual motion fretting were adhesive and abrasive wear. At higher loads the main wear mechanisms were a combination of adhesive wear, abrasive wear, cracking and lubrication of human bone tissue debris [46].

The comparison between radial fretting and dual motion fretting of cortical bone was made by Gao et. al. in 2010 [47]. They found that dual motion fretting produced more damage and more wear debris than radial fretting. Radial fretting produced significantly more cracks than dual motion fretting and the abundance of cracks was dependant on the bone microstructure. Radial fretting could thus be used to study the crack propagation of bone [47].

The bio-response of bone to the micro-motion in vivo has also been studied in the past. In the earliest researches concluded that micro-motion inhibited bone ingrowth into implant and led to the formation of a fibrous membrane between the implant/bone interface. The anchorage of bone to implant was therefore compromised [48] [49].

In 1973, Cameron et. al. presented the idea of a threshold micro motion [50]. They suggested that fibrous membrane does not form at interface upto a certain value of micro-motion amplitude.

In 1986, Pillar et. al. confirmed the existence of the threshold micro-motion. Their research led to the conclusion that micro motion values of 150 μm to 500 μm could lead to damage and membrane formation [51].

In 1993, Brunski detailed his ideas on the problems of overloading and micro-motion on dental implant/bone interface [52]. He suggested that “based on evidence so far, as a rule of thumb: relative motion of more than 100 microns should be avoided”. He also suggested that the threshold micro-motion cannot be fixed because it depends on the implant system.

In 2003, Gapski et. al. reviewed the effect of immediate implant loading [53]. He agreed with the past concepts of threshold micro-motion and Brunsk's "rule of thumb". Based on these, they differentiated two different kinds of micro-motions: tolerable and deleterious. They concluded that primary implant stability is the most important factor affecting immediate implant loading [53].

It can be concluded that tribological properties of a dental implant material play an important role in its performance and the tribological problems that can occur when a dental implant is integrated into the biological system need to be analyzed and solved before deeming a material suitable for this particular application.

3. EXPERIMENTAL PROCEDURE

3.1. Materials and methods

The materials used for tribological test were tantalum samples and artificial bone material (epoxy resin reinforced by glass fibers). The preparation of these materials has been described in sub chapters of this topic (3.1.1 & 3.1.2).

3.1.1. Tantalum sample preparation

Tantalum sheets (T1-9000-D73), of purity 99.95% and thickness of 0.5 mm, were obtained from the supplier Testbourne. Tantalum samples were prepared by cutting the sheets to dimensions of 20 x 25 mm with a cutting machine. The burrs formed on the edge of the samples, from cutting the metal sheet, were removed by using grinding paper of grit size 320. In order to prepare the sample surface for anodization, both sides of the samples were polished on grinding papers of grit size size 250, 320, 500, 800, 1200 and 2000, 2500 and 4000. Six conditions were defined for the treatment of the samples and these are summarized in Table 3.1.

Table 3.1. Treatment conditions of tantalum samples

No.	Treatment
1	Polished (reference)
2	Polished and Anodized at potential of 15 V in H_2SO_4:HF (9:1)
3	Polished and Etched in HNO_3:HF (1:1) solution (reference)
4	Etched and Anodized at 15 V in H_2SO_4:HF (9:1)
5	Etched and Anodized at 25 V in H_2SO_4:HF (9:1)
6	Etched and Anodized at 50 V in H_2SO_4:HF (9:1)

As Table 3.1 shows, two samples were used as reference. They differed in terms of their surface preparation i.e. mechanical polishing and chemical etching. The Ta sheets supplied had poor surface quality hence etching was employed to remove scratchs and irregularities from the surface. But since etching introduces pitting at the micron level on the metal surface, the effect of this micro porosity on the friction of the textured surface was also studied. Hence the mechanically polished sample was required for comparison in this case. The samples were etched in an acid solution consisting of nitric acid and hydrofluoric acid (1:1) for two minutes. Extreme care needed to be taken during the

etching process due to the use of highly corrosive liquids. The samples immersed in the solution were carefully stirred after every 30 seconds in order to ensure uniform etching. After etching treatment the samples were washed with distilled water and air dried.

The samples underwent two-sided anodization as the schematic of the electrochemical setup show in Figure 3.1. As the name suggests, two-sided anodization causes both sides of a sample to be textured. This setup was designed at University of Minho by Professor Sandra Carvalho. The electrolyte solution used for anodization consisted of H_2SO_4 and HF in the ratio 9:1. The voltage was supplied by an electronic voltage source.The test was performed at galvanostatic conditions. The samples were fixed on a metallic sample holder and care was taken to immerse the samples only half way in, so as to avoid contact between the sample holder and the strong electrolyte as this could affect the anodization process. As soon as the sample was immersed in the electrolyte solution, the voltage source was turned on. During the experiment the electrolyte was constantly stirred by a magnetic stirrer in order to ensure uniform texturing on the sample surface. The electrochemical process ran for two minutes, after which the voltage source was turned off. The sample was removed and washed with distilled water to remove residue acid. A few nanotubes of Ta_2O_5 usually form during anodization and when the objective is to obtain nanopores, these need to be removed. Hence, the anodized sample was placed in another small beaker filled with distilled water and ultrasonic cleaning was performed for 15 minutes in order to remove the nanotubes.

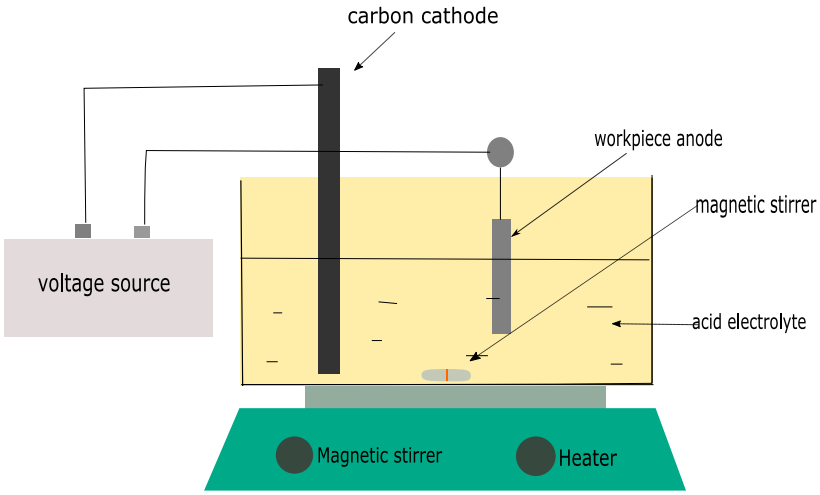

Figure 3.1. Schematics of experimental setup for two-sided anodization of Ta metal.

The samples were anodized at three different voltages in order to achieve different pore sizes on the oxide layer. Increasing the potential increases the pore size [23] as stated earlier in the state of the art. It should also be noted that increasing the voltage also increases the oxide film thickness [55]. Hence, the samples anodized at 50 V had a thicker oxide layer with a distinct grey-green color. Tantalum oxide tends to exhibit different colors depending on the applied voltage, and at around 50 V the oxide film usually exhibits a grey-green colour [56]. This phenomena was not observed on the surface of the samples anodized at 15 V and 25 V. The surface of the different samples was analyzed under an optical microscope and the results have been discussed in Chapter 4.1.

3.1.2. Bone material

The artificial bone material that was used for friction tests was a composite of epoxy resin reinforced with glass fibers, as it had mechanical properties most closely resembling cortical bone. The artificial bone material was supplied by Sawbones. The composite was prepared for thr friction test by cutting it into a cylinder which had a diameter of 8 mm and a thickness of 2 mm. The composite samples were then glued to solid steel cylinders that had been prepared to fit into the sample holders of the friction test equipment. Figure 3.2 shows a prepared artificial bone sample and the placement of the samples in the friction testing machine.

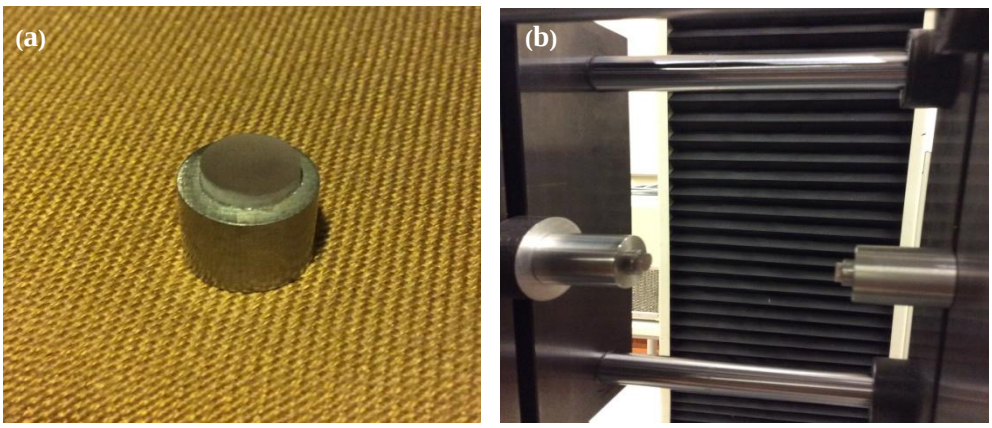

Figure 3.2. (a) Prepared artificial bone sample (b) Artificial bone samples placed in the friction test equipment.

3.2. Characterization Techniques

The prepared tantalum samples were characterized by various techniques. The surface of the samples was inspected under an optical microscope and images were captured with a camera attached to the microscope (Canon A620).

Field Emission Scanning Electron Microscopy (Zeiss Merlin Gemini 2) was used to observe the morphology of the sample surfaces in order to compare the textured surfaces with polished and etched surfaces, to measure the pore size of nano pores formed on the surface of samples anodized at different potentials and to determine the uniformity of nano-texturing obtained on the sample surface after anodization treatment.

X-ray Diffraction (PANalytical X'Pert PRO) was used to analyze the crystallographic structure of the etched and anodized tantalum samples. Bragg-Brentano X-ray diffraction was performed in conventional (θ-2θ) mode (scan range $20^\circ < 2\theta < 85^\circ$, step size $2\theta = 0.04^\circ$, scan step time 3 seconds and Cu Kα1 radiations ($\lambda = 1.54060$ Å).

Hardness measurements were made by using the Vickers hardness method (Struess Duramin) in order to determine change in hardness due to developed of oxide layer of different thickness. Hardness tests were performed with a diamond shaped indenter at two different, 25 and 100 g.

The surface roughness of tantalum samples was measured using a 3-D profilometry (alicona INFINITE FOCUS) in order to determine changes in the surface roughness after etching and anodization treatment. The roughness measurements were also performed on samples that have been kept in saliva at 37 ˚C for three days.

The tribological characterization was done by using a friction coefficient measurement device which was originally developed in CEMUC. An image of the setup and the schematics are shown in Figure 3.2. The setup was operated by a standard tensile testing machine with electronic control of cross-head motion [54].

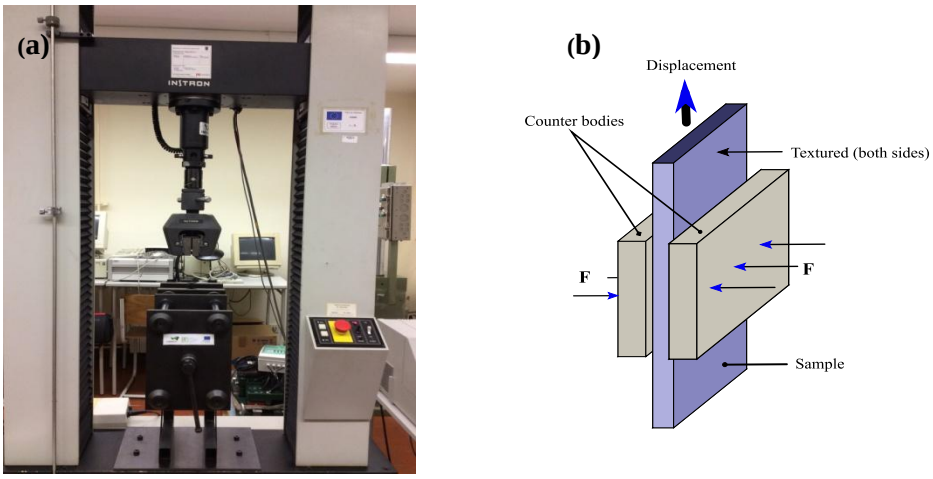

Figure 3.3. (a)The friction coefficient measurement setup and (b) schematics of the friction test

As the schematics in Figure 3.3 show, the tantalum sample was placed in the sample holder in the center and the cortical bone mimicking composite, epoxy resin reinforced with glass fiber, was fixed into holders located on opposite side of the sample, and brought into contact with the tantalum metal surface. The so called 'sandwich' was clamped together firmly and a normal force (F) of 250 N was applied. In all experiments the samples were displaced at a contant speed of 1 mm/min in the vertical direction. The resulting force vs. displacement relationship was plotted. The experiment was stopped when the plot achieved steady state. The plot was used to obtain three parameters: contact rigidity, static friction force and dynamic friction force . The slope of the initial linear part of the plot represented the rigidity of the interfacial contact, the maximum force represented the force required to initiate sliding. This force is used to calculate the static friction coefficient which will be discussed in the chapter: results and discussion. After the maximum force was reached the plot showed a decrease in force, until a constant force is reached. This was represented by a steady state on the plot. The constant force represented the dynamic force i.e. the amount of force required to slide the sample after the sample surface had overcome the static friction. This parameter was used to calculate the dynamic friction coefficient. These three parameters were compared for samples treated at different conditions in order to obtain information regarding their friction properties. The friction tests were conducted at room temperature in both dry and wet conditions. For the wet condition, the samples were immersed in artificial saliva and placed in an isothermal bath which was kept at a constant temperature of 37 ˚C. The samples were kept in artificial saliva for three days in order to analyze the ageing effect of saliva on the friction results.

The artificial saliva solution used in the experiments was prepared by using the guidelines given in a publication by Darvell [57]. Prior to placing the samples in saliva, wetting contact angle measurements were made to determine the change in wettability of tantalum surface after surface treatment. Contact angle measurements were made with the instrument dataphysics Contact Angle System OCA. The droplet volume was 9 µl and the liquid used for comparison was water AS. Three measurements were taken for each sample in order to ensure repeatability of results.

Wear marks formed at the sliding contact region on the sample surfaces, during friction tests, were observed under an optical microscope in order to analyze and compare degree of wear caused by sliding on the different treated tantalum surfaces.

4. RESULTS AND DISCUSSION

4.1. Surface Imaging (Optical Microscopy)

After the Ta samples were prepared, their surfaces were analyzed under an optical microscope (LEICA DM4000) . Images of the Ta surfaces, captured by the camera connected to the microscope (LEICA MC120 HD) are shown in Figure 4.1.

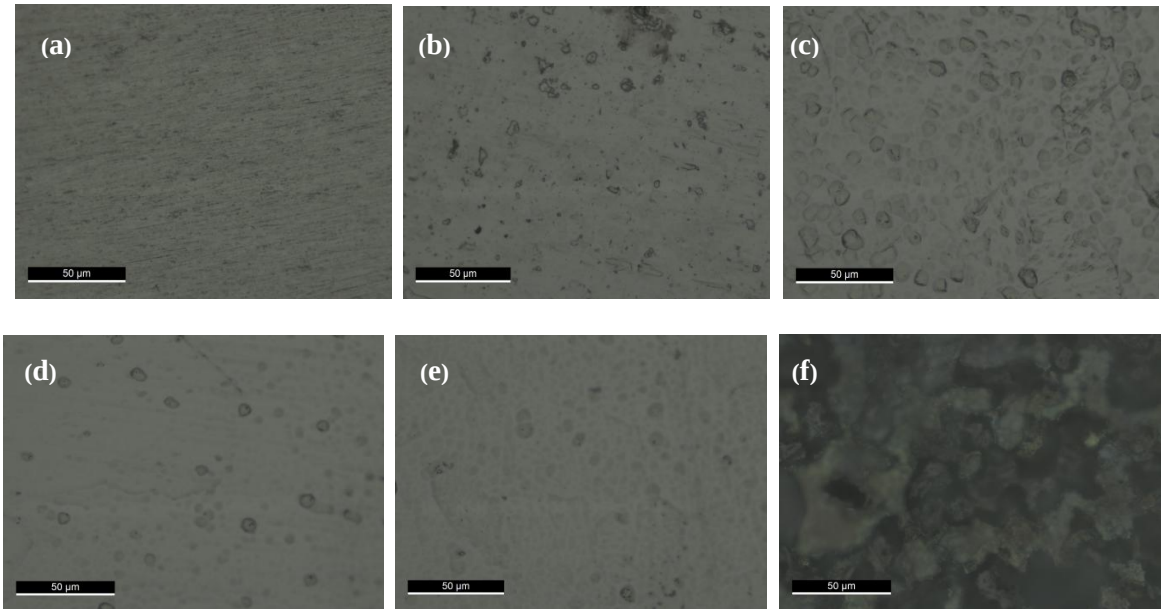

Figure 4.1. Surface images of Ta samples obtained from optical microscope. (a) Ta-Polished, (b)Ta-Polished and anodized at 15 V, (c) Ta-Etched, (d) Ta-polished, etched and anodized at 15 V (e) Ta-polished, etched and anodized at 25 V, (f) Ta-polished, etched and anodized at 50 V

Figure 4.1(a) shows that the polished sample surface was preferablly oriented in one direction but other than than it was featureless and smooth. Figure 4.1(b) shows the effect of anodization after mechanical polishing. The surface showed a few features that looked like micro pits. These could have occured due to non uniform anodic attack by strong acidic electrolyte that occurred on the deformed polished surface. The oxide layer may have been etched more strongly in some parts than others. Figure 4.1(c) shows the Ta sample that was etched in a concentrated solution of HNO3:HF (1:1). The surface shows micro pits formed due to etching. The micro pits were, on an average, less than 25 µm in size. Anodization treatment at a potential of 15 and 25 V, after etching, caused a reduction of the micro-pits and smoothened out the surface more, as can be observed in Figure 4.1(d) & (e). Anodization at 50 V led to the development of a thicker oxide film which exhibited

the characteristic grey-ish coloring (Figure 4.1 (f)) that usually develops when Ta2O5 is formed at 50 V [56].

Surface morphology was examined at higher magnifications to obtain nano features, using SEM. The results are presented in Chapter 4.2.

4.2. Surface Morphology

The SEM images given in Figure 4.2 show the surface of tantalum samples treated at different conditions. Figure 4.2 (a) shows the tantalum surface of polished and of polished and etched surfaces at 50,000 X magnification. In both cases texturing at the nano level was not observed. The figure shows that the surface is featureless in the un-anodized sample surfaces. The surface of the tantalum sample which was polished and anodized at a potential of 15V shows ordered porosity on the surface, with the average pore size of 25 nm. The supplied tantalum sheets had poor surface quality and surface preparation by mechanical polishing did not seem adequate as evident from the uneven surface in the image, Figure 4.2 (b). In order to overcome this problem and improve the surface condition, etching was also performed prior to anodization. Figure 4.2 (c) shows the SEM image of the tantalum sample etched and anodized at 15V. The surface shows highly ordered nano-porosity with an average pore size of 25 nm. The difference in the etched surface and the un-etched surface can be observed from the images. Etching the sample successfully decreased the irregularities on the surface and improved surface quality. Figure 4.2 (d) shows the surface of sample etched and anodized at a potential of 25 V. The increases in pore size can be observed from the image. This treatment resulted in an average pore size of 45 nm.

Figure 4.2 (e) shows the surface of the sample etched and anodized at a potential of 50 V. The high voltage resulted in an increase in Ta_2O_5 oxide layer thickness. The growth of the oxide layer was not uniform, as evident from the irregular topography of the surface from Figure 4.2 (f). The pore size increased and the shape of the pores became irregular. The average pore size achieved after this treatment was 65 nm.

EDS (Energy-dispersive X-ray spectroscopy) analysis was also performed in order to obtain information about elements present on the anodized surfaces. The EDS result, presented in Annex A, shows that the only elements present on the surface of the

anodized samples were tantalum and oxygen. SEM images obtained at magnification of 200000X are given in Annex B.

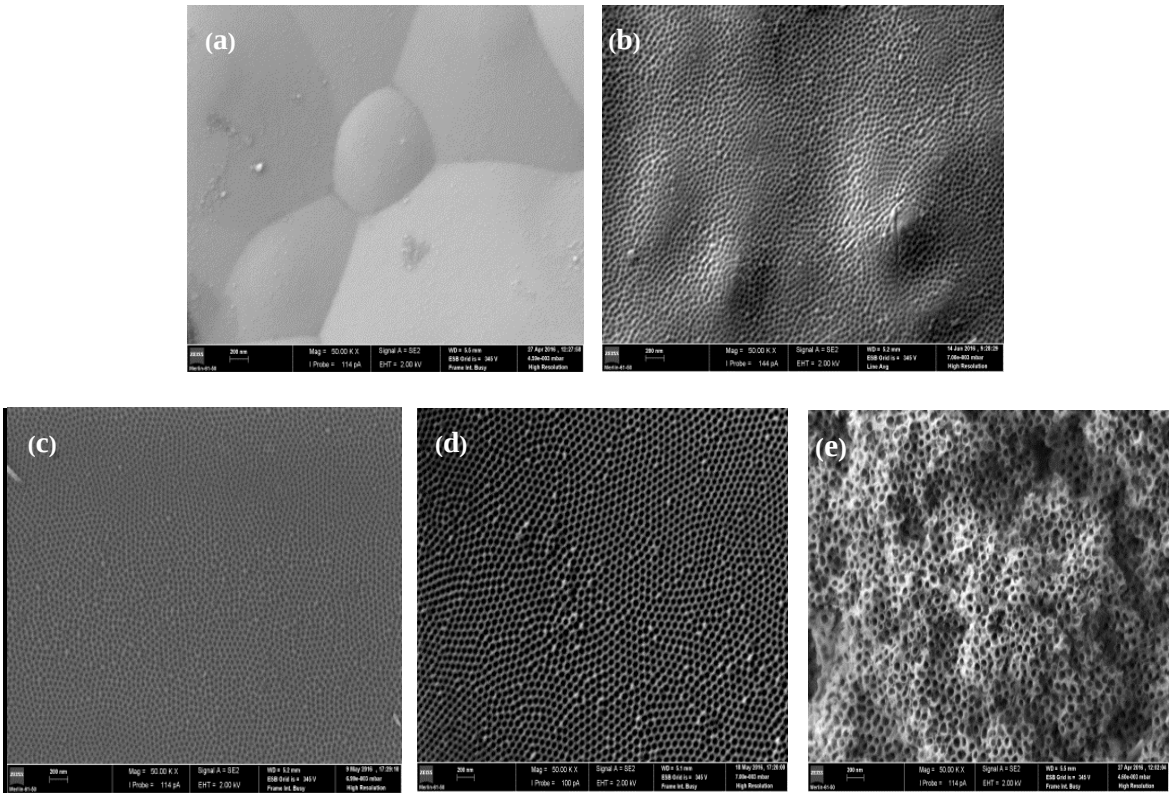

Figure 4.2. SEM images (50000X magnification) of Ta surfaces treated at different conditions (a) polished and etched (b) Polished and anodized at 15 V (c) Polished, etched and anodized at 15 V (d) Polished, etched and anodized at 25 V (e) Polished, etched and anodized at 50 V

4.3. Crystal Structure

The X-ray diffraction patterns obtained for tantalum samples treated at different conditions are shown in Figure 4.3. All the samples, with the exception of the samples anodized at 50 V, exhibit diffraction peak positions that are associated with BCC structured alpha phase Tantalum metal (ICDD card no: 00-004-0788). However, the xrd patterns of the etched and anodized samples showed a difference in peak intensities.

The XRD pattern associated with the polished Ta sample (Figure 4.3(a)) was in agreement with the reference xrd pattern (ICDD card no: 00-004-0788). However, the XRD pattern of the sample that was anodized at a potential of 15 V and the etched Ta sample (Figure 4.3(b)&(c)) showed a significant decrease in intensity of the peak associated with (110) plane and an increase in the intensity of the peaks associated with the (200) and (211) planes. A possible explanation for this is preferential etching of the (110) plane which caused its intensity to decrease and since the other planes were now present in

larger quantity in the xrd analysis region, their xrd intensities became higher. The phenomena of differential etching has been observed before and it is caused due to a difference in the packing density and orientation of different planes [58]. The electrolyte composition used for this anodization process was used before in a research study and the phenomenon of differential etching as a function of crystallographic orientation of tantalum grains was reported [59].

Performing the anodization process after etching seemed to have led to preferential etching of the (110) and (200) planes, as indicated from the decrease in their respective intensities observed from Figure 4.3(d). Furthermore, increasing the anodization voltage caused an overall decrease in the intensity of the peaks associated with α-Ta as deduced from Figure 4.3 (e). This is a result of a greater contribution by the Ta_2O_5 film as its thickness increased. This oxide film is generally known to be amorphous [60] [61]. The increase in oxide film thickness occurred due to anodization at a higher potential. Hence, the distance between the xrd rays and the α-Ta surface increased, causing most of the x-rays to be absorbed by the amorphous oxide layer, leading to a decrease in α-Ta peaks intensities. The XRD pattern associated with the sample anodized at 50V did not have the peaks associated with α-Ta, which indicates a lack of long range crystallinity. Hence, it could be deduced that the thickness of the oxide layer had increased to the point that the XRD pattern observed is predominantly contributed by the Ta_2O_5 film.

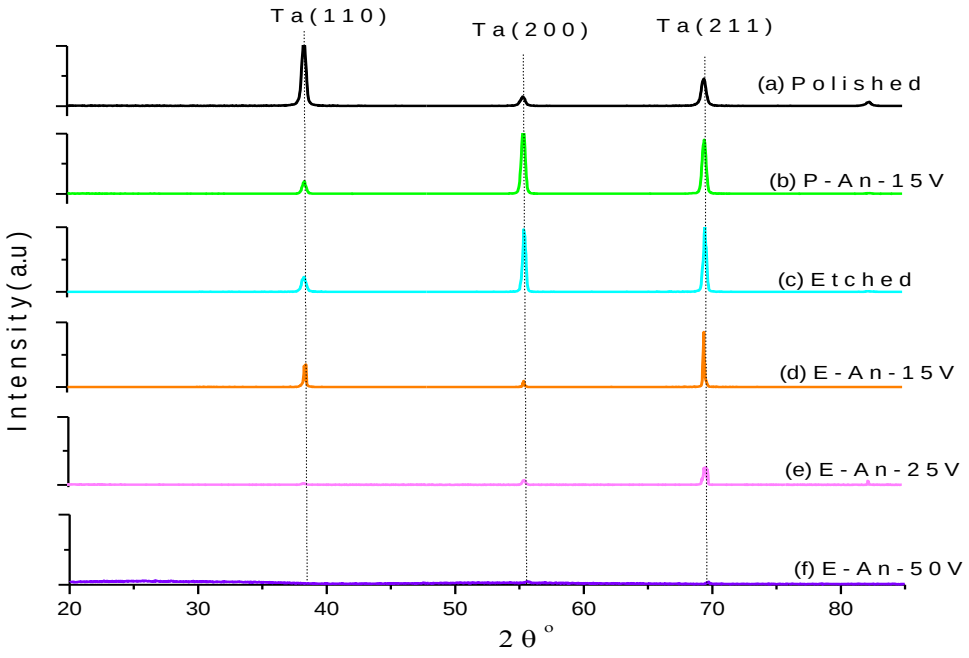

Figure 4.3. XRD patterns of Ta samples treated at different conditions (a) Pure Ta with polished surface (b) Ta metal polished and anodized at 15V (c) Ta metal polished and etched (d) Ta metal polished, etched and anodized at 15V (e) Ta metal polished, etched and anodized at 25V (f) Ta metal polished, etched and anodized at 50V

4.4. Hardness

Table 4.1 shows Vickers hardness measurements, of Ta samples, obtained at two different indenter loads. The hardness value of polished sample, measured using the smaller indentation load, was 224 HV. However when a higher load was used, the hardness value measured was smaller and closer to the values obtained for all the other samples. The reason for a higher hardness obtained at lower indentation load is that mechanical polishing may have led to surface hardening due to the plastic deformations that occurred on the surface during the treatment. When higher indentation load of 100 g was used, the indentation depth increased and crossed through the hardened surface. Hence the hardness value measured at higher indentation load was of the un-deformed Ta surface.

All other Ta samples, with the exception of the one anodized at 50 V, showed similar hardness values at both high and low indentation loads. The oxide layer on samples anodized at 15 and 25 V was penetrated by the indenter and the final hardness measurement was of the Ta metal. Hence, the values of hardness were similar. The sample that was anodized at 50 V showed a lower hardness at indentation load of 25 g. This sample developed a higher thickness of oxide layer and the indenter was not able to penetrate this film completely. Hence the hardness measurement also had a major contribution from this amorphous oxide film which had a lower hardness than Ta metal. However, the hardness value increased to match the values obtained from other samples when a higher indentation load of 100 g was used. This means that the oxide layer had been penetrated and the hardness value obtained was from Ta metal. This information can be used to conclude that the oxide layer thickness has an effect on the surface hardness of the samples and this could possibly affect their tribological behavior.

Table 4.1. Vicker hardness measurements of Ta surfaces treated at different conditions

Sample	HV (25 g)	HV (100 g)
Polished	224	149.3
Polished and Anodized at 15 V	150.6	149.8
Etched	152	150.1
Polished, etched and Anodized at 15 V	150.8	149.7
Polished, etched and Anodized at 25 V	150.7	148.9
Polished, etched and Anodized at 50 V	100.8	150.4

4.5. Wetting behavior

Wetting contact angle measurements on Ta surfaces were made by using artificial saliva as wetting fluid. Table 4.2 shows the average contact angle measurements obtained for the samples. The measurements were very similar to each other with very small deviations. It could be deduced that the nano texturing had not caused a significant change in the wettability of Ta surfaces when saliva was used as liquid.

However possible experimentation could be performed in the future, to test the time dependent wettability of the nano textured surfaces.

Table 4.2. Wetting contact angle measurements of Ta samples with artificial saliva as wetting fluid

Sample	Wetting Contact angle (art. saliva)
Polished	80.3
Polished and Anodized at 15 V	83.4
Etched	83.9
Polished, etched and Anodized at 15 V	80.8
Polished, etched and Anodized at 25 V	80.6
Polished, etched and Anodized at 50 V	83.7

4.6. Surface Roughness

The results of 3-D profilometry performed on Ta samples treated at different conditions are presented in Table 4.3. Roughness results were obtained in both dry conditions and after immersion in saliva.

4.6.1. Surface roughness in dry condition

The polished untreated sample had the lowest surface roughness compared to the other samples, which was expected since its surface had not undergone any surface texturing treatment. The Rz surface roughness values for this sample were very small as can be seen from Table 4.3. The Ta sample that was anodized after polishing, without etching treatment, had a higher surface roughness than the polished sample. Even though no etching treatment had been performed on the surface, the anodization process itself could be called an electrochemical etching process. Mechanical polishing is achieved by plastic deformation which changes the crystal structure on the surface more or less intensively by disturbing the orientation. The quality of surface is poorer compared to a chemically polished surface. Anodization is sensitive to the nature of the surface. The

uneven polished layers are etched off more easily than the undisturbed structure beneath them. This uneven etching results in an increase in surface roughness. The increase in Rz value indicated that this surface had more peaks and valleys than the polished sample. However, this electrochemical treatment seemed to be less aggressive than chemical etching, as indicated from the Rz value of this sample, which were smaller compared to the chemically etched sample.

The chemically etched Ta sample had a significantly higher surface roughness compared to the polished surface and polished & anodized surface. Etching in a strong acid solution of nitric acid and hydrofluoric acid resulted in micro pitting on the surface and consequently, in an increase in surface roughness.

The samples that were polished, etched and anodized at 15 V had a higher surface roughness than the polished and anodized sample at the same potential. The acid etching treatment improved the quality of the surface by removing scratches and irregularities. But it introduced micropits on the surface and anodization treatment at a low voltage of 15 V did not significantly affect the micro scale surface roughness of the etched sample. However, at higher anodization potentials smaller Rz value was obtained, of samples anodized at 25. This could be due to the increase in the intensity of electrochemical attack which would have an increased smoothening effect and lead to a decrease in surface roughness. An abnormally small Rz value was obtained at 50 V.

4.6.2. Surface roughness after immersion in saliva

The profilometry measurements of Ta samples that had been kept in artificial saliva showed a difference in surface roughness values compared to the data obtained in dry conditions. It would be hard to determine what changes occurred due to immersion in saliva that caused the change in surface roughness. It requires further research and experimentation.

Table 4.3. Surface roughness data obtained for Ta samples treated at different conditions

Surface Treatment of Ta sample	Dry condition	Wet condition
	Rz (µm)	Rz (µm)
Polished	0.75	0.68
Polished and anodized at 15V	7.22	5.26
Etched in acid solution	8.82	7.88
Polished, etched and anodized at 15V	9.71	10.54
Polished, etched and anodized at 25V	4.37	4.91
Polished, etched and anodized at 50V	3.34	8.76

4.7. Friction Behavior

The resulting force vs displacement plots obtained from the friction tests performed on the tantalum samples are displayed in Figure 4.4. The figure presents a graphic view of how the Ta surfaces behaved during the friction test.

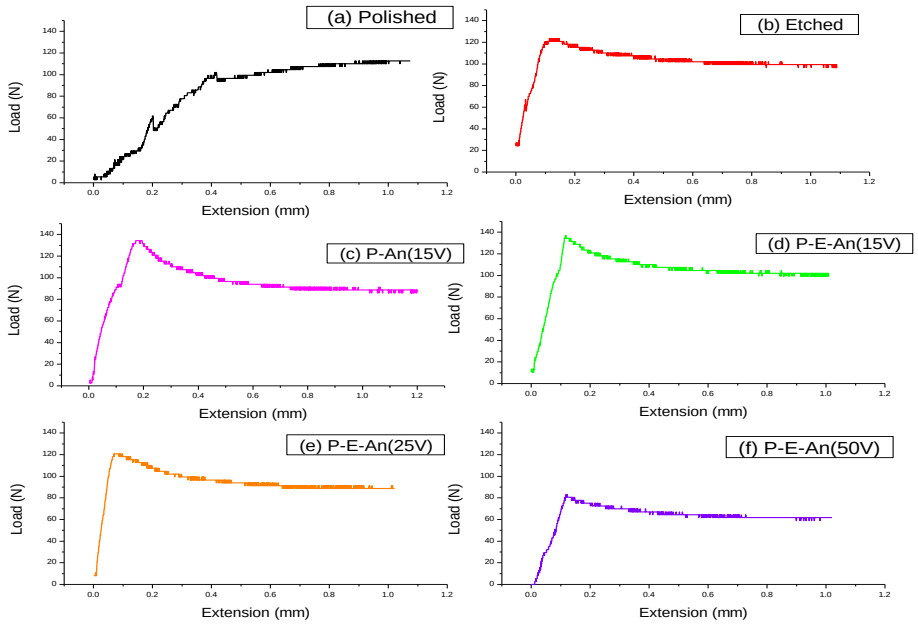

Figure 4.4. Force vs. Displacement graphs resulted from friction tests of Ta surfaces (in contact with glass fiber epoxy composite). (a) Ta polished (b) Ta polished and etched (c) Ta polished and anodized at 15 V (d) Ta polished, etched and anodized at 15 V (e) Ta polished, etched and anodized at 25 V (f) Ta polished, etched and anodized at 50 V

All the plots, with the exception of the one for polished Ta, exhibited the characteristics of a typical static friction plot. The maximum static friction force, as well as the decrease in force to a constant steady state, could clearly be observed on the plots. During the friction test the Ta sample was in contact with artificial bone material on both

sides. Consequently the friction results were contributed by two interfaces of Ta sample/artificial bone material. In order to obtain the result from a single interface the results simply needed to be divided by two. The stiffness of the Ta surface/artificial bone contact, static friction force and dynamic force values obtained from each plot were divided by 2. The results are presented in Table 4.4.

Table 4.4. Friction parameters obtained from friction plots of Ta samples treated at different conditions

Sample	Rigidity (N/mm)	Static friction force (N)	Dynamic friction force (N)
Polished	123.155	51.175	56.3
Polished and anodized at 15 V	495.845	67.415	44.485
Polished and Etched	501.835	61.92	49.67
Polished, etched and anodized at 15V	543.225	68.53	51.87
Polished, etched and anodized at 25V	975.02	60.395	44.71
Polished, etched and anodized at 50V	401.48	41.605	31.025

The static and dynamic friction coefficient was obtained by using equation 1 and 2.

$$\mu_s = \frac{F_{max}}{N}; \qquad [1]$$

$$\mu_d = \frac{F_{steady\ state}}{N} \qquad [2]$$

μ_s = static friction coefficient
μ_d = dynamic friction coefficient
F_{max} = maximum force obtained from friction plot
$F_{steady\ state}$ = Average force at steady state
N = Normal load

The theoretical applied normal load in all experiments was 250 N and it was fixed by using the electronic control connected to the load cell. Linear calibration of the load cell was performed, in order to measure the real applied load. The calculated sensitivity of the load cell was 0.67 N/mV and consequently the real applied normal load was 167.63 N. This was the value of normal load used in Equation 1. The static and dynamic friction coefficient data is given in Table 4.5.

Table 4.5. Friction coefficients of Ta samples treated at different conditions

Sample	Static friction coefficient (μ_s)	Dynamic friction coefficient (μ_d)
Polished	0.31	0.34
Polished and anodized at 15 V	0.40	0.27
Polished and Etched	0.37	0.29
Polished, etched and anodized at 15V	0.42	0.31
Polished, etched and anodized at 25V	0.36	0.26
Polished, etched and anodized at 50V	0.25	0.19

4.7.1. Static Friction Behavior

The static friction coefficient holds the most relevance in the study of the tribological behavior of the textured Ta surface as a dental implant material, as it is directly related to mechanical interlocking efficiency. The dental implant should be able to form a good mechanically interlocking at the contact region with bone and micro motion should be minimized, the static friction coefficient is desired to be high. Hence this friction parameter was given the most focus in the discussion of the tribological results.

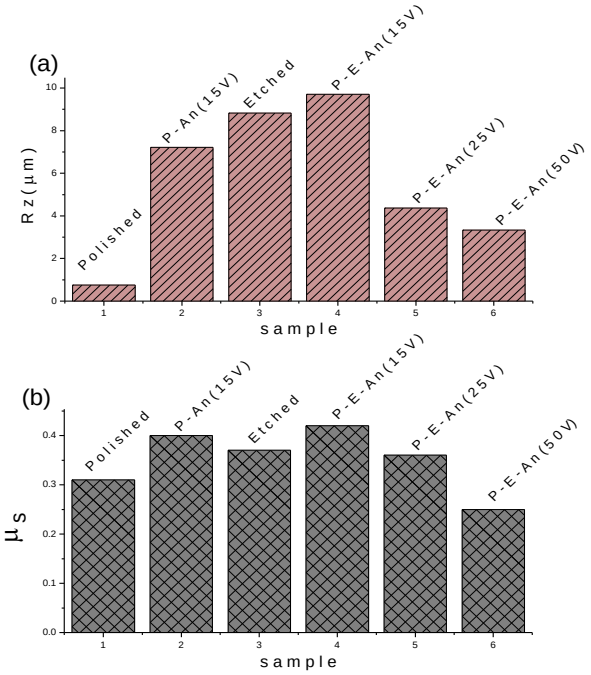

Figure 4.5. (a) The mean peak to valley height of roughness profile (Rz) and (b) static friction coefficient (μ_s) of Ta surfaces treated at different conditions (P=Polished, E=Etched, An=Anodized)

The static friction coefficient has been discussed in relation to the surface roughness, in order to study the hypothesis made in this research, that surface roughness

has the most dominant effect on the friction properties of textured Ta surfaces. Figure 4.5 shows the surface roughness and static friction coefficient of Ta samples treated at different conditions.

The polished sample showed a very small static friction force peak and the static friction force was smaller than the dynamic friction force (Figure 4.4 (a)). This occurred due to the low Rz value associated with this sample (Table 4.3) i.e. the mean peak to valley height was small. Hence it could be deduced that the polished sample surface failed to mechanically interlock effectively with the artificial bone material and slippage occurred readily. Hence, in Figure 4.5 it can be seen that the surface roughness value is the lowest, but the static friction coefficient (μ_s) value is higher than that of the sample anodized at 50 V. Even though the value of static friction coefficient was higher, the static friction regime was very small. Therefore the polished sample could be called an abnormal friction result.

The sample that was mechanically polished and anodized at 15 V had a static friction coefficient value of 0.4 (Table 4.5). This could be correlated to the Rz value of 7.22 µm (Table 4.3) which means that the surface had asperities that formed mechanical interlocking effectively with the glass fiber epoxy surface. This high surface roughness may have developed due to the non uniform growth of tantalum oxide that occurred as a result of non uniform electrochemical etching during anodization. The surface may have developed heterogeneities such as hardness, surface shear strength etc. which contributed to its friction behavior. The tantalum sheets that were supplied had poor surface quality. The only treatment done on this sample that was polished and anodized at 15 V, for improving the surface quality was mechanical polishing, hence some defects may have remained on the surface and these could have contributed to the static friction.

The change in static friction coefficient of the etched and anodized samples was similar, in trend, to change in their surface roughness (Figure 4.5). The chemically etched sample surface had a smaller mean peak to valley height of roughness profile (Rz) than the sample that was etched and anodized at 15 V. It also showed a smaller coefficient of friction. The anodized sample also had a higher contact rigidity compared to the etched sample (Table 4.4). This could have been due to the development of the amorphous tantalum oxide layer. This oxide layer would exhibit different surface properties than the Ta surface. A previous research study showed that the hardness and elastic modulus of tantalum oxide layer varied with its thickness and thin oxide layers are capable of withstanding large elastic deformations without failure [62].

The sample anodized at 25 V showed even higher rigidity. Anodization at 25 V resulted in a greater film thickness and the amorphous film showed greater elasticity at the contact region. Hence it could be deduced that the oxide film thickness of this sample was within the limit of high elasticity defined in the research work mentioned in the previous paragraph [62]. However, it showed a lower static friction coefficient than the etched sample and the sample anodized at a lower potential of 15 V. This decrease in the static friction was attributed to the low surface roughness of this sample. The Rz value of this sample was significantly smaller compared to the etched and the anodized samples; hence it may have formed poorer mechanical interlocking. Despite the significant difference in the surface roughness, the static friction of this sample was not significantly smaller than the one anodized at 15 V or the chemically etched sample. This may have been because of the higher rigidity at contact region caused due to the good elasticity of the film, which hindered initiation of slippage. It has been observed that at increasing oxide film thickness (>100 nm), this elastic behavior decreases and more plastic strain is observed [62]. From Table 4.4, comparing the etched and anodized samples it can be seen that contact rigidity increased i.e. the etched sample had the lowest contact rigidity, which increased for the sample anodized at 15 V and the highest was achieved for the sample anodized at 25 V. However, contact rigidity decreased for the sample that was anodized at 50 V. The Rz value of this sample was also the lowest, compared to the other anodized samples. Consequently, this sample exhibited the lowest static friction coefficient. This sample had the highest oxide film thickness. From the SEM image in Figure 4.2 (e) it was observed that the oxide layer was not homogenously formed. The surface was non uniform and the pores were larger and irregular. This surface also exhibited lower hardness value. These factors may have contributed towards the sample's poor friction performance compared to the other anodized samples.

The surface roughness of the different Ta sample surfaces seemed to be the dominant factor in determining their static friction behavior. However, other contributions such as surface adhesion and the effect of the surface properties of oxide layer were not studied.

4.7.2. Dynamic Friction Behavior

The dynamic friction behavior represents how the sample surface would behave when it start sliding. Although sliding of a dental implant is not desired, it is

important to have knowledge about the dynamic friction behavior as it helps in understanding the micro motion behavior of the implants and also their failure mechanisms.

The polished sample showed the highest dynamic friction coefficient compared to the treated samples. This could be explained in terms of the surface polishing which led to an increase in surface flatness. This was supported by the very small Rz surface roughness value of polished sample (Table 4.3), which indicated a very flat surface. This led to an increase in the contact area between Ta and the glass fiber epoxy composite. A higher sliding force was required to drag the Ta surface over the composite's surface. However, the contact rigidity was the smallest, compared to other samples (Table 4.4). Despite the high dynamic friction coefficient, the absence of any effective static contact and consequently the failure of the un-textured sample to form an effective mechanically interlocking with artificial bone and hence resulted in small contact rigidity.

Figure 4.6 shows the comparison of static and dynamic friction coefficients of the etched and the anodized samples. The dynamic friction coefficient was smaller than the static friction coefficient in all cases. This is a typical friction behavior that surfaces exhibit. In the initial stage of sliding, the surface asperities undergo deformation and wear i.e. the running-in effect. Sliding could be described as a polishing phenomenon as it leads to surface smoothening resulting from wear. The Ta sample surfaces were worn due to sliding contact with glass fiber epoxy composite and the wear marks were observable with the naked eye.

The Ta surface anodized at 15 V after mechanical polishing had a lower dynamic friction coefficient than the surface anodized at the same potential after etch treatment. This could be related to the quality of oxide film that formed on both surfaces. The anodized Ta surface may have worn off more easily due to the poor adherence of the oxide film to the metal surface. Scratch tests could provide a more detailed insight into this argument but this would have to be left for future work due to the shortage of time. However this argument makes sense as the wear track of this sample showed a shinier surface than the etched sample, hence a higher degree of wear (Chapter 4.8).

The samples anodized at higher potentials had lower dynamic friction coefficients compared to the samples anodized at 15 V. These thicker oxide layers maye have been more easily worn away. The surface shear strength may have changed as surface texturing occurred at higher potential. A greater intensity of electrochemical attack on the

surface at higher potentials may have reduced the surface strength. This would cause surface wear to occur at lower dynamic friction forces.

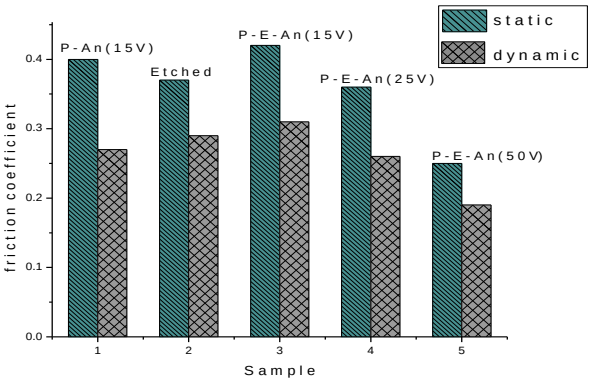

Figure 4.6. Static and dynamic friction coefficients of Ta surfaces treated at different conditions (P=Polished, E=Etched, An=Anodized)

4.7.3. Static Friction Behavior in Artificial Saliva (Dry vs. Wet)

Past research has shown that artificial saliva has shown conflicting results. In some cases it has caused a decrease in static friction while in other cases it led to an increase in static friction. Static friction tests performed on orthodontic wires in a similar manner as the one performed in this research led to varying results. Kusy et al. [63] for example, concluded that artificial saliva was an inadequate replacement for human saliva and hence any experiments related to it as incorrect. Andreasen and Quevedo [64] suggested that the saliva does not play a significant role, while Read-Ward et al. [65] concluded that the presence of human saliva had an inconsistent effect on static friction and sliding mechanics. Furthermore, Baker et al. [66] reported that saliva had a lubricating effect whereas Stannard et al. [67] reported that saliva increased friction. Therefore a common effect of artificial saliva on friction properties has not been reported as there have been conflicted reports of the adhesive and lubricating effect of saliva. In the previous reports the artificial saliva was sprayed onto the sample during the test to maintain constant wetting condition. In this thesis, the effect of artificial saliva was studied by immersing the samples in artificial saliva solution for three days at a constant temperature of 37 ˚C, after which the samples were removed and friction tests were performed. The hypothesis that was being tested in this research was that saliva acts as a lubricant and the lubricating effect should improve in the nano textured samples as the nano pores could act as saliva

reservoirs. The friction behavior of Ta samples treated at different conditions showed interesting results. Figure 4.7 shows the friction behavior of Ta samples tested in dry and wet condition.

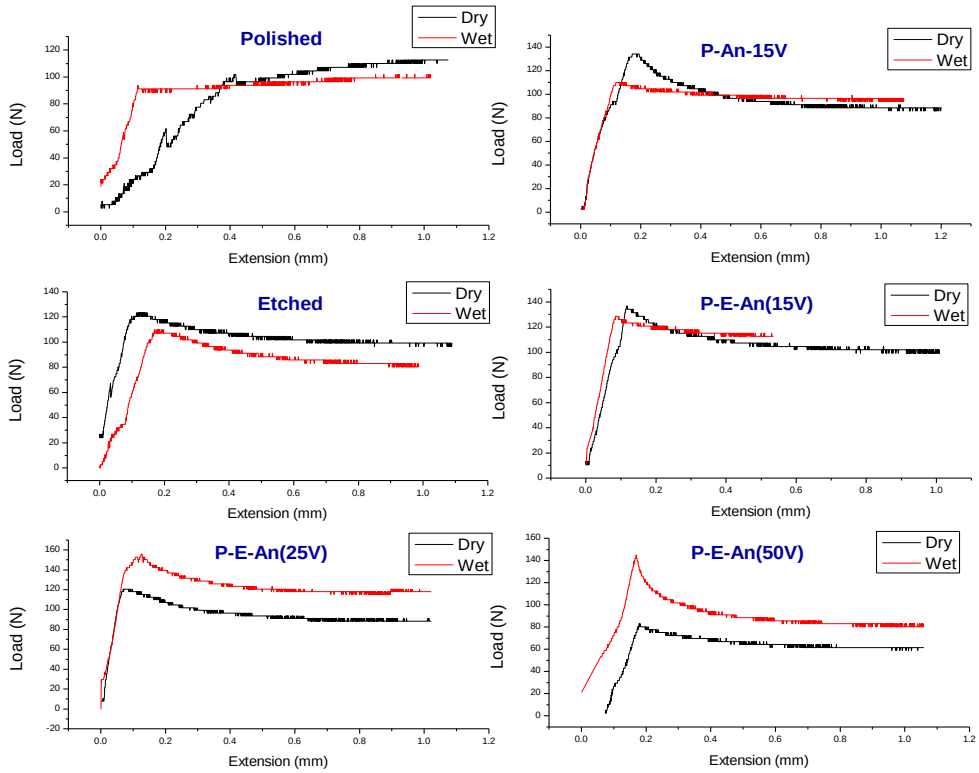

Figure 4.7. Friction graphs of Ta samples in dry and wet conditions (P=Polished, E=Etched, An=Anodized)

The figure shows that the friction graph of the polished sample did not exhibit any static friction region and the graph itself did not represent typical friction behavior. The friction plot of etched sample in wet condition showed that the static and dynamic friction force were lower compared to dry condition. The samples anodized at 15 V showed that the dynamic friction increased in wet condition, but the static friction decreased. But the samples anodized at 25 V and 50 V showed that both the static and dynamic friction force increased. The static friction coefficient data of Ta samples obtained in dry and wet conditions is compiled in Table 4.6.

Table 4.6. Static friction coefficient data of Ta samples in dry and wet conditions

Sample	μ_s (Dry)	μ_s (Wet)

Polished	0.31	--
Polished and anodized at 15 V	0.40	0.33
Polished and Etched	0.37	0.35
Polished, etched and anodized at 15V	0.42	0.38
Polished, etched and anodized at 25V	0.36	0.46
Polished, etched and anodized at 50V	0.25	0.43

Table 4.6 shows that the sample polished and anodized at 15 V, the etched sample and the sample that was anodized at 15 V after etching showed a decrease in static friction coefficient. However, the sample that was anodized at 25 V, after polishing and etching, showed a significant increase in static fricition coefficient in wet condition. A similar result was seen for the case of Ta sample anodized at 50 V. It is hard to provide a specific reason for this difference as there could be various factors that may have contributed to this significant increase in static friction coefficient. It could have been that chemical deposits from the saliva solution, such as NaCl, formed more readily on these surfaces and raised the friction coefficient. More testing is required to reach a solid conclusion.

4.7.4. Dynamic friction behavior in dry vs. wet conditions

The anodized Ta samples behaved quite differently from static conditions when sliding initiated. The Table 4.7 provides the compiled data of dynamic friction coefficients, of Ta samples, obtained in dry and wet conditions. The polished and etched samples had lower dynamic friction coefficients in wet condition. However the anodized samples showed an increase in dynamic friction. Table 4.7 shows that the friction plots of samples anodized at 15 V achieved steady state regime at higher forces, even though the static friction force was slightly lower. The samples anodized at 25 V and 50 V had a significant increase in dynamic friction. It is also interesting to note that the friction coefficient of sample anodized at 50V was still lower than the other etched and anodized samples. This could be attributed to the non uniform oxide layer that formed on the surface at this potential and the decreased hardness of the surface due to increased oxide thickness.

Dynamic friction behavior did not show dependence on the Rz surface roughness. Hence, in discussing the conclusion of the friction analysis the static friction behavior was given focus.

Table 4.7. Dynamic friction coefficients of Ta samples in dry and wet conditions

Sample	μ_d (Dry)	μ_d (Wet)
Polished	0.34	0.29
Polished and anodized at 15 V	0.27	0.29
Polished and Etched	0.29	0.25
Polished, etched and anodized at 15V	0.31	0.34
Polished, etched and anodized at 25V	0.26	0.35
Polished, etched and anodized at 50V	0.19	0.25

4.7.5. Static friction vs. Surface roughness

After discussing the static and dynamic friction behavior of Ta samples treated at different conditions, a clear relationship between the surface roughness and static friction behavior needed to be established in order to test the hypothesis that surface roughness plays a dominant role in determining the static friction behavior of Ta surface. Hence a scatter graph of static friction coefficient vs surface roughness (Rz) of Ta surfaces, in both dry and wet conditions, was plotted and a line of best fit was used to obtain the trend in the scatter of points (Figure 4.8). Majority of the data points are evenly distributed about the trend line and majority of the data points lay close to the line, which shows that the static friction coefficient is influenced by surface roughness.

Hence from this research study it could be deduced that the surface roughness affects the static friction behavior of textured Ta surfaces. It is, however, important to state that this was a preliminary research study that was conducted to test a hypothesis and the results showed promising potential if this research study is extended and more experimental testing and characterization is performed.

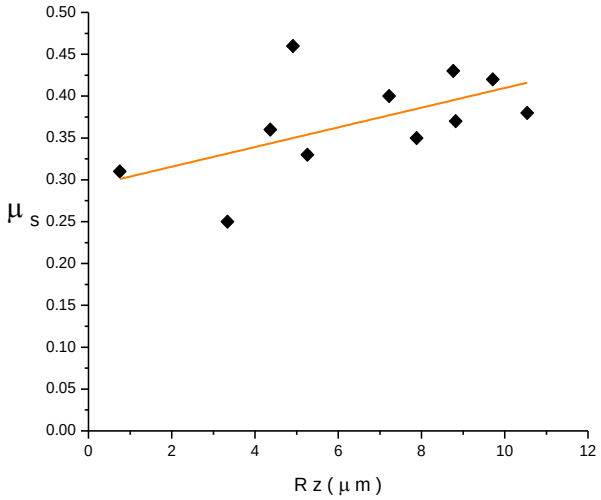

Figure 4.8. Relationship between surface roughness (Rz) and static friction coefficient (μ_s) of Ta samples treated at different conditions

4.8. Wear analysis

When the static friction at the Ta/glass fiber epoxy contact region was overcome, the Ta sample started to slide. The Ta samples exhibited wear at the sliding contact region. The wear regions were observed under an optical microscope and the degree of wear on the surface of different samples was compared.

4.8.1. Dry condition

The optical microcope images showed that the anodized Ta surfaces exhibited different degree of wear compared to the untreated Ta surfaces. Figure 4.9 (a) shows the surface of the polished Ta sample. The image shows a circle of contrast in the middle, which is the sliding contact region. Sliding did not seem to have caused significant degree of wear on the polished Ta surface. Figure 4.9 (b) shows the surface of Ta sample anodized at 15 V after mechanical polishing. The sliding contact region is much more visible and brighter in this image. This surface was scratched and worn to a higher degree compared to the polished Ta surface.

Figure 4.9 (c) shows the surface of chemically etched Ta sample. The central circular region of sliding contact region can be observed in the image. This region showed that sliding on the etched Ta surface had to caused high degree of wear. The area surrounding the sliding region shows bright spots on the etched surface. Etching usually occurs at

different rates at grains of different orientations, grain boundaries and defects. It also leads to some micro pitting on the metal surface. The micro pits on etched Ta surface were observed in Figure 4.1 (c). Thus etched metal surface usually shows bright and dark contrast regions. The image in Figure 4.9(c) was taken at low magnification, hence the bright regions are only visible as bright spots on the surface.

Figure 4.9(d) & (e) show that the sliding contact region in surfaces anodized at 15 and 25 V respectively, had a brighter sliding contact region compared to etched surface. The sliding region on these surfaces show higher degree of scratching and wear compared to etched Ta surface. The anodized samples had a nano-textured Ta_2O_5 surface. In Chapter 4.3 (Crystal structure) it had been discussed that the oxide layer was amorphous (Figure 4.3). Hence the surface properties of the anodized samples would be expected to be different. The amorphous oxide would be expected to be more brittle and have different shear strength than Ta metal. Due to the anodic attack, the textured surfaces would also be expected to have higher stresses. These and other surface properties might have made them more susceptible to wear than un-anodized metal surface, hence the higher degree of wear and scratching. The scratches are oriented in the direction of sliding

Figure 4.9 (f) shows the surface of Ta sample anodized at 50 V. The image shows different colors compared to images of other samples in Figure 4.9, the bright spots appearing yellower and the sliding region appearing grey-green. This was caused by the characteristic grey-green colored oxide film that developed at 50 V (discussed previously in Chapter 4.1, in reference to Figure 4.1 (f)). Figure 4.9 (f) shows that the sliding contact region does not show a clear distinct shape. The scratches on the surface are oriented in the direction of sliding and the surface with the bright yellow spots could possibly be the exposed etched surface after some oxide film has worn away.

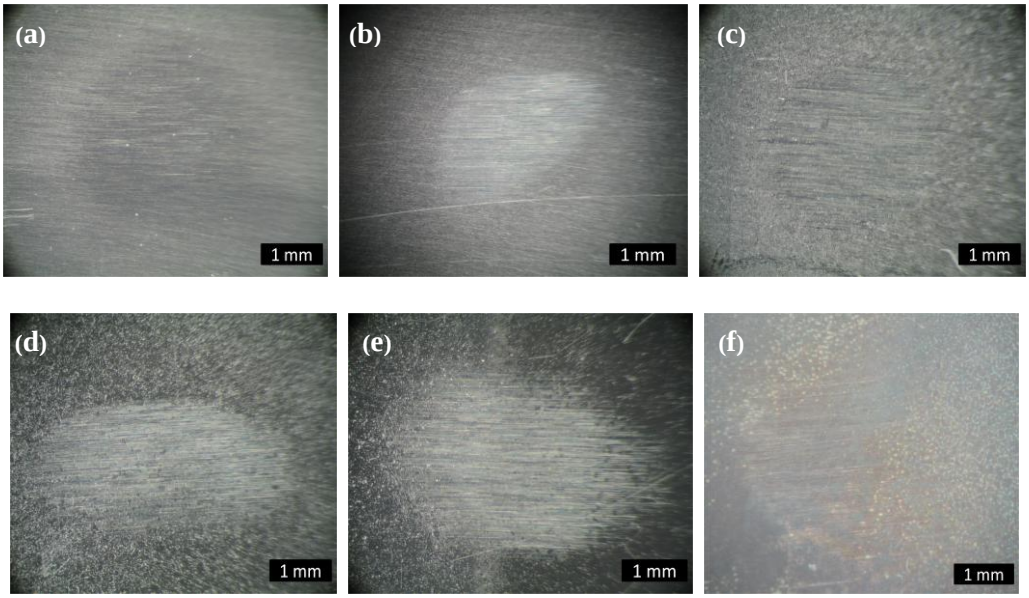

Figure 4.9. Wear marks on Ta surfaces after friction test in dry conditions (a) Ta-polished (b) Ta-polished and anodized at 15 V (c) Ta-etched (d) Ta-polished, etched and anodized at 15 V (e) Ta-polished, etched and anodized at 25 V (f) Ta-polished, etched and anodized at 50 V

4.8.2. Wet condition

The wear marks in Figure 4.10 were formed on Ta surface that had been immersed in artificial saliva for three days prior to friction tests. The polished and etched sample showed low wear at sliding region (Figure 4.10 (a)&(c)), which was similar to the observations made on these surfaces in dry conditions (Figure 4.9 (a)&(c)). Ta sample, that was anodized after mechanical polishing, showed a bright circular sliding region. The surface showed considerable scratching and wear.

The samples that were etched and anodized at 15 and 25 V (Figure 4.10 (d)&(e)) also showed bright sliding regions. The scratches and wear in the region was easily observable. The sliding region on the sample anodized at 50 V (Figure 4.10 (f)) was very visible under the microscope. The oxide layer had clearly been worn away as the bright metal surface was exposed at the sliding region, in clear contrast to the dull grey-green oxide surface in the surrounding regions.

The anodized surfaces in both dry and wet conditions showed a higher degree of wear than un-anodized surfaces. The textured tantalum oxide clearly had surface properties which made it more vunerable to surface wear than Ta metal. Anodic attack possibly induced surface stresses. Ta samples anodized at different potentials underwent different intensity of chemical attack by the strong electrolyte. This could affect the degree of surface stresses induced on the oxide surface and the surface shear strength. Figure 4.10

(f) shows that the oxide film was worn off. Hence the adhesion of the oxide films formed at different anodic potential may have also differed.

The wear marks obtained in wet condition were different in shape and size. But this difference in wear mark dimensions was not relevant. The variation in dimensions of sliding region was expected, as Ta sample alignment during the test could vary for each test and the test was stopped when the friction graph showed steady state regime. Hence, sliding time was not a constant. Subsequently the dimensions of the sliding contact region were different.

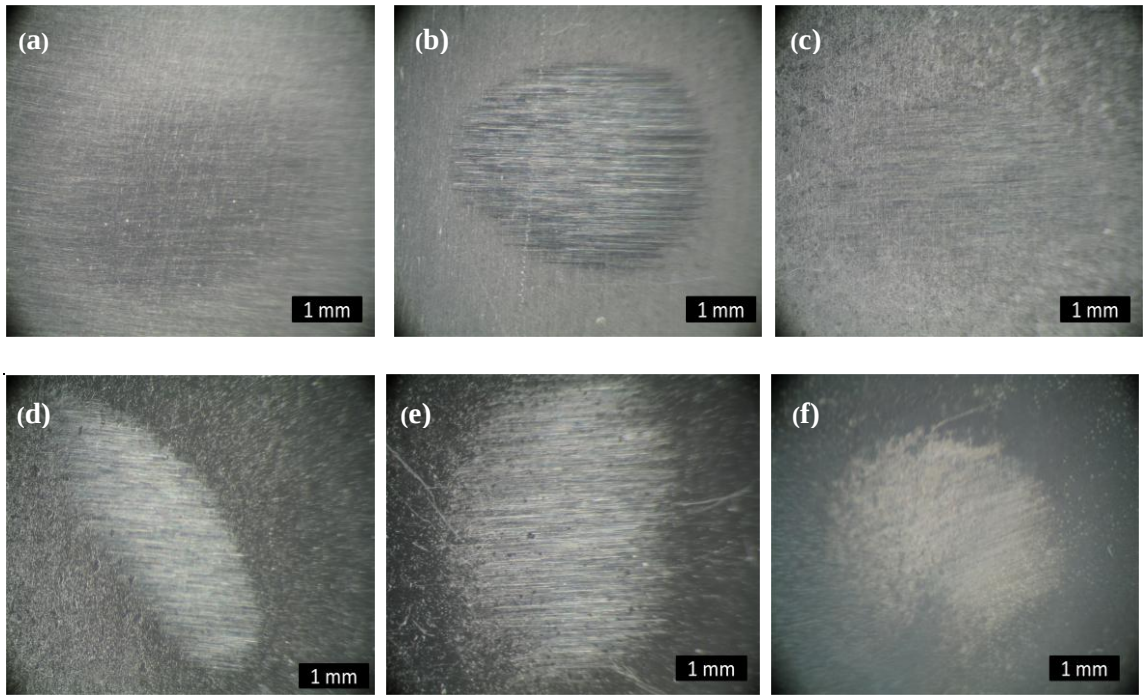

Figure 4.10. Wear marks on Ta surfaces after friction tests in wet condition. (a) Ta-polished (b) Ta-polished and anodized at 15 V (c) Ta-etched (d) Ta-polished, etched and anodized at 15 V (e) Ta-polished, etched and anodized at 25 V (f) Ta-polished, etched and anodized at 50 V

CONCLUSIONS

In this thesis the tribological properties of nano textured tantalum were studied. Anodization method was used to introduce highly ordered nano pores on tantalum surface. Three different potentials, 15, 25 and 50 V, were used in anodization in order to obtain three diferent pore diameters on the nano dimpled surface. Three different average pore sizes were obtained at different potentials, SEM images showed that highly ordered nano texturing had been achieved by the electrochemical process.

XRD patterns of the treated Ta samples showed that the tantalum oxide film was amorphous and preferential etching had occured on the treated surfaces. The hardness results showed that the amorphous oxide layer is softer than the metal and the hardness tends to change with oxide thickness as effect of the metal on the overall hardness decreases.Wetting contact angle measurements showed that there was no significant change in the wetting behavior of treated and untreated Ta surfaces.

3-d profilometry measurements showed that anodization influenced the micro-surface roughness (Rz).The static friction coefficient showed an almost linear dependancy on the micro surface roughness. Dynamic friction coefficient did not show a clear relationship to surface roughness. The anodized Ta surfaces had nano textured amorphous oxide layer and showed a higher degree of wear than the un-anodized Ta surfaces.

It can be concluded that nano texturing by anodization treatment caused the surface roughness to change on the micron level. The surface roughness was a major contributor to the static friction behavior of the untreated and treated Ta surfaces. Hence, when deciding the optimum nano texture, by anodization, for biological performane of Ta dental implant it is also important to assess its friction behavior, as it plays an important role in defining the performance of the dental implant when it is inserted into the jaw and brought into contact with bone.

FUTURE WORK

1. The friction tests on nano textured Ta surfaces will be performed with real bone material to obtain a more realistic result of the friction behavior of the textured Ta surfaces as dental implants.

2. Study the history of the materials before sample preparation

3. The Ta surfaces will be anodized at more magnitudes of voltage in order to achieve a wider range of pore size on the textured surface. This could provide more information and data regarding the relationship between surface roughness and friction behavior of nano textured Ta surfaces.

4. Scratch tests will performed to study the adhesion of oxide film formed at different voltages during anodization, as this could provide more information regarding the wear behavior of nano textured Ta surfaces.

5. The experiments will be repeated for higher number of times to obtain a more statistically improved data.

6. The time dependent wetting behavior of nano textured Ta surfaces, with artificial saliva, will be studied.

7. The fretting behavior of the nano textured Ta surfaces will be studied.

BIBLIOGRAPHY

[1] Z. Zhou, H. Yu,, J. Zheng,, L. Qian, Y. Yan, *Dental biotribology*, New York, Springer, 2013.

[2] J. Black, "Biologic performance of tantalum", *Clinical Materials*, vol.16, 1994, p.167-173.

[3] H. Matsuno, A. Yokoyama, F. Watari, M. Uo, T. Kawasaki, "Biocompatibility and osteogenesis of refractory metal implants, titanium, hafnium, niobium, tantalum and rhenium", *Biomaterials*, vol.22, 2001, p.1253-1262.

[4] M. A. Ballo, O. Omar, W. Xia, A. Palmquist, "Dental Implant Surfaces – Physicochemical Properties, Biological Performance, and Trends". *Implant Dentistry - A Rapidly Evolving Practice*, 2011.

[5] P. I. Branemark, U. Breine, B. Johansson, P. J. Roylance, H. Rockert, J. M. Yoffey, "Regeneration Of Bone Marrow", *Acta Anatomica*, vol.59, 1964, p.1-46.

[6] C. Nelson, "Factors Affecting the Success of Dental Implants", *Implant Dentistry - A Rapidly Evolving Practice*, 2011.

[7] T. Ebert, "Dental Implants Progression", *Dentalimplantsprogression.blogspot.pt*, 2012, <http://dentalimplantsprogression.blogspot.pt/> [accessed 24 February 2016].

[8] A. Wennerberg, T. Albrektsson, "On implant surfaces: a review of current knowledge and opinions", *The International Journal of Oral & Maxillofacial Implants*, vol.25, no.1, 2010, p.63-74.

[9] L. Le Guéhennec, A. Soueidan, P. Layrolle, Y. Amouriq, "Surface treatments of titanium dental implants for rapid osseointegration", *Dental Materials*, vol.23, no.7, 2007, p.844-854.

[10] A. Wennerberg, T. Albrektsson, C. Johansson, B. Andersson, "Experimental study of turned and grit-blasted screw-shaped implants with special emphasis on effects of blasting material and surface topography", *Biomaterials*, vol.17, no.1, 1996, p.15-22.

[11] A. Wennerberg, T. Albrektsson, B. Andresson, "Bone tissue response to commercially pure titanium implants blasted with fine and coarse particles of aluminum oxide", *The International Journal of Oral & Maxillofacial Implants*, vol.11, no.1, 1996, p.38-45.

[12] M. J. Jackson, A. Waqar (Eds.), "Anodization: A Promising Nano-Modification Technique of Titanium-based Implants for Orthopedic Applications", *Surface Engineered Surgical Tools and Medical Devices*, 2007, p.21-47.

[13] K. De Groot, R. Geesink, C. Klein, P. Serekian, "Plasma sprayed coatings of hydroxylapatite", *Journal of Biomedical Materials Research*, vol. 21, no.12, 1987, p.1375-1381.

[14] T. Webster, J. Ejiofor, "Increased osteoblast adhesion on nanophase metals: Ti, Ti6Al4V, and CoCrMo", *Biomaterials*, vol. 25, no. 19, 2004, p.4731-4739.

[15] Y. Sul, C. Johansson, Y. Jeong, T. Albrektsson, "The electrochemical oxide growth behaviour on titanium in acid and alkaline electrolytes", *Medical Engineering & Physics*, vol. 23, no. 5, 2001, p.329-346.

[16] J. Choi, R. Wehrspohn, J. Lee, J. Gosele, "Anodization of nanoimprinted titanium: a comparison with formation of porous alumina", *Electrochimica Acta*, 49, 16, 2004, p.2645-2652.

[17] W. Baun, "Formation of porous films on titanium alloys by anodization" *Surface Technology*, vol.11, no.6, 1980, p.421-430.

[18] M. Okada, K. Tajima,Y. Yasusei, K. Yoshimura, "Self-Organized Formation of Short TiO2 Nanotube Arrays By Complete Anodization of Ti Thin Films", *Physics Procedia*, vol.32, 2012, p.714-718.

[19] A. Jaroenworaluck, D. Regonini, C.R. Bowen, R. Stevens, "Nucleation and early growth of anodized TiO2 film". *Journal of Materials Research*, vol.23, no.8, 2008, p.2116-2124.

[20] R. Beranek, H. Hildebrand, P. Schmuki, "Self-Organized Porous Titanium Oxide Prepared in H[sub 2]SO[sub 4]/HF Electrolytes", *Electrochemical and Solid-State Letters*, vol.6, no.3, 2003, p.B12.

[21] P. Roy, S. Berger, P. Schmuki, "TiO2 Nanotubes: Synthesis and Applications", *Angewandte Chemie International Edition*, vol.50, no.13, 2011, p.2904-2939.

[22] C. Grimes, G. Mor, *TiO_2 nanotube arrays*. Dordrecht, Springer, 2009.

[23] D. Gong, C. Grimes, O. Varghese, W. Hu, R. Singh, Z. Chen, E. Dickey, "Titanium oxide nanotube arrays prepared by anodic oxidation", *Journal of Materials Research*, vol.16, no.12, 2001, p.3331-3334.

[24] S. Minagar, C. Berndt, J. Wang, E. Ivanova, C. Wen, "A review of the application of anodization for the fabrication of nanotubes on metal implant surfaces", Acta *Biomateralia*, vol.8, no.8, 2012, p.2875-2888.

[25] Q. Cai, L. Yang, Y. Yu, "Investigations on the self-organized growth of TiO_2 nanotube arrays by anodic oxidation", *Thin Solid Films*, vol.515, no.4, 2006, p.1802-1806.

[26] G. Mor, K. Shankar, M. Paulose, O. Varghese, C. Grimes, "Enhanced Photocleavage of Water Using Titania Nanotube Arrays", *Nano Letters*, vol.5, no.1, 2005, p.191-195.

[27] V. Balla, S. Banerjee, S. Bose, A. Bandyopadhyay, "Direct laser processing of a tantalum coating on titanium for bone replacement structures", *Acta Biomaterialia*, vol.6, no.6, 2010, p.2329-2334.

[28] V. Balla, S. Bose, N. Davies, A. Bandyopadhyay, "Tantalum—A bioactive metal for implants", *The Journal of The Minerals, Metals & Materials Society*, vol.62, no.7, 2010, p.61-64.

[29] S. Jafari, B. Bender, C. Coyle, J. Parvizi, P. Sharkey, W. Hozack, "Do Tantalum and Titanium Cups Show Similar Results in Revision Hip Arthroplasty?", *Clinical Orthopaedics and Related Research®*, vol.468, no.2, 2009, p.459-465.

[30] Q. Lu, S. Mato, P. Skeldon, G. Thompson, D. Masheder, H. Habazaki, K. Shimizu, "Anodic film growth on tantalum in dilute phosphoric acid solution at 20 and 85°C", *Electrochimica Acta*, vol.47, no.17, 2002, p.2761-2767.

[31] I. Sieber, H. Hildebrand, A. Friedrich, P. Schmuki, "Initiation of tantalum oxide pores grown on tantalum by potentiodynamic anodic oxidation", *Journal of Electroceramics*, vol.16, no.1, 2006, p.35-39.

[32] W. Wei, J. Macak, P. Schmuki, "High aspect ratio ordered nanoporous Ta2O5 films by anodization of Ta", *Electrochemistry Communications*, vol.10, no.3, 2008, p.428-432.

[33] N. Allam, X. Feng, C. Grimes, "Self assembled fabrication of vertically oriented Ta_2O_5 nanotubes arrays, and membranes thereof, by one-step tantalum anodization", *Chemistry of Materials*, vol.20, no. 20, 2008, p.6477-6481.

[34] I. Hasan, L. Keileg, M. Staat, G. Wahl, C. Bourauel, "Determination of the frictional coefficient of the implant-antler interface: experimental approach", *Biomedizinische Technik/Biomedical Engineering*, vol.57, no.5, 2012, p.359-363.

[35] P. Predcki, B. Auslaender, J. Stephan, V. Mooney, C. Stanitski, "Attachment of bone to threaded implants by ingrowth and mechanical interlocking", *Journal of Biomedical Materials Research*, vol.6, no.5, 1972, p.401-412.

[36] D. Puleo, A. Nanci, "Understanding and controlling the bone–implant interface", *Biomaterials*, vol.20, no.23-24, 1999, p.2311-2321.

[37] J. Galante, J. Jacobs, "Clinical Performances of Ingrowth Surfaces", *Clinical Orthopaedics and Related Research*, vol.276, 1992, p.41-49.

[38] S. Cook, K. Thomas, H. Haddad, "Histologic Analysis of Retrieved Human Porous-Coated Total Joint Components", *Clinical Orthopaedics and Related Research,*vol. 234, 1988, p.90-101.

[39] C. Engh, J. Bobyn, A. Glassman, "Porous-coated hip replacement. The factors governing bone ingrowth, stress shielding, and clinical results", *Journal of Bone and Joint Surgery*, vol.69, no.1, 1987, p.45-55.

[40] H. Bulaqi, M. Mousavi, F. Geramipanah, H. Safari, M. Paknejad, "Effect of the coefficient of friction and tightening speed on the preload induced at the dental implant complex with the finite element method", *The Journal of Prosthetic Dentistry*, vol.113, no.5, 2015, p.405-411.

[41] L. Carlsson, T. Rostlund, B. Albrektsson, P. Branemark, "Osseointegration of titanium implants", *Acta Orthopaedica*, vol.57, no.4, 1986, p.285-289.

[42] P. Buchert, P. Vaughn, T. Mallory, T. Engh, J. Bobyn, "Excessive metal release due to loosening and fretting of sintered particles on porous-coated hip prostheses: Report of two cases", *Journal of Bone and Joint Surgery*, vol.68, no.4, 1986, p.606-609.

[43] H. Yu, Z. Cai, Z. Zhou, M. Zhu, "Fretting behavior of cortical bone against titanium and its alloy" *Wear*, vol.259, no.7-12, 2005, p.910-918.

[44] S. Gao, Y. Zhang, Z. Zhu, H. Yu, "Micromotions and combined damages at the dental implant/bone interface", *International Journal of Oral Science*, vol.4, no.4, 2012, p.182-188.

[45] H. Yu, H. Quan, Z. Cai, S. Gao, M. Zhu, "Radial Fretting Behavior of Cortical Bone Against Titanium", *Tribol Lett*, vol.31, no.2, 2008, p.69-76.

[46] H. Yu, S. Gao, S. Cai, H. Quan, M. Zhu, "Dual-motion fretting behavior of mandibular cortical bone against pure titanium", *Tribology International*, vol.42, no.9, 2009, p.1365-1372.

[47] S. Gao, Z. Cai, H. Quan, M. Zhu, H. Yu, "Comparison between radial fretting and dual-motion fretting features of cortical bone", *Tribology International*, vol.43, no.1-2, 201, p.440-446.

[48] K. Søballe, E. Hansen, H. B-Rasmussen, P. Jorgesen, C. Bunger, "Tissue ingrowth into titanium and hydroxyapatite-coated implants during stable and unstable mechanical conditions", *Journal of Orthopaedic Research*, vol.10, no.2, 1992, p.285-299.

[49] Y. Akagawa, M. Hashimoto, N. Kondo, K. Satomi, T. Takata, H. Tsuru, "Initial bone-implant interfaces of submergible and supramergible endosseous single-crystal sapphire implants", *The Journal of Prosthetic Dentistry*, vol.55, no.1, 1986, p.96-100.

[50] H. Cameron, R. Pilliar, I. Macnab, "The effect of movement on the bonding of porous metal to bone", *Journal of Biomedical Materials Research*, vol.7, no.4, 1973, p.301-311.

[51] R. Pilliar, J. Lee, C. Maniatopoulos, "Observations on the Effect of Movement on Bone Ingrowth into Porous-Surfaced Implants", *Clinical Orthopaedics and Related Research*, vol.208, 1986, p.108-113.

[52] J. Brunski, "Avoid pitfalls overloading and micromotions of intraosseous implants" *Dental Implantology Update*, vol.4, no.10, 1993, p.77-81.

[53] R. Gapski, H. Wang, P. Mascarenhas, N. Lang "Critical review of immediate implant loading", *Clinical Oral Implants Research*, vol. 14. no.5, 2003, p.515-527.

[54] M. Costa, C. Leitao, A. Ramalho, D. Rodrigues, "Local improvement of structural steels high-friction properties by friction stir texturing", *Journal of Materials Processing Technology*, vol.217, 2015, p.272-277.

[55] A. Radisic, G. Oskam, P. Searson, "Influence of Oxide Thickness on Nucleation and Growth of Copper on Tantalum", *Journal of The Electrochemical Society*, vol.151, 2004, p.C369.

[56] C. Sheng, Y. Cai, E. Dai, C. Liang, "Tunable structural color of anodic tantalum oxide films", *Chinese Physics* B, vol.21, 2012, p.088101.

[57] B. Darvell, "The development of an artificial saliva for in vitro amalgam corrosion studies", *Journal of Oral Rehabilitation*, vol.5, 1978, p.41-49.

[58] Y. Zhang, D. Chen, *Multilayer integrated film bulk acoustic resonators*, Heidelberg, Springer, 2013, p.65.

[59] H. El-Sayed, S. Singh, P. Kruse, "Formation of Dimpled Tantalum Surfaces from Electropolishing", *Journal of the Electrochemical Society*, vol.154, 2007, p.C728.

[60] S. Maeng, L. Axe, T. Tyson, A. Jiang, "An Investigation of Structures of Thermal and Anodic Tantalum Oxide Films", *Journal of the Electrochemical Society*, vol.152, 2005, p.B60.

[61] M. Momeni, M. Mirhosseini, M. Chavoshi, A. Hakimizade, "The effect of anodizing voltage on morphology and photocatalytic activity of tantalum oxide nanostructure", *Journal of Materials Science: Materials in Electronics*, vol.27, 2015, p.3941-3947.

[62] S. Dub, V. Starikov, "elasticity module and hardness of niobium and tantalum anode oxide films", *Functional Materials*, vol.14, 2007, p.347-350.

[63] R. Kusy J. Whitley, M. Prewitt, "Comparison of the frictional coefficients for selected archwire-bracket slot combinations in the dry and wet states", *Angle Orthodontist*, vol.61, no.4, 1991, p.293–302

[64] G. Andreasen, F. Quevedo, "Evaluation of friction forces in the 0·022 × 0·028 edgewise bracket in vitro", *Journal of Biomechanics*, vol.3, 1970, p.151-160.

[65] G. Read-Ward, S. Jones, E. Davies, "A comparison of self-ligating and conventional orthodontic bracket systems.", *British Journal of Orthodontics*, vol. 24, 1997, p.309-317.

[66] K. Baker, L. Nieberg, A. Weimer, M. Hanna, "Frictional changes in force values caused by saliva substitution", *American Journal of Orthodontics and Dentofacial Orthopedics*, vol.91, 1987, p.316-320.

[67] J. Stannard, J. Gau, M. Hanna, "Comparative friction of orthodontic wires under dry and wet conditions", *American Journal of Orthodontics*, vol.89, 1986, p.485-491.

ANNEX A – SEM-EDS SPECTRUM OF ANODIZED TANTALUM SURFACE

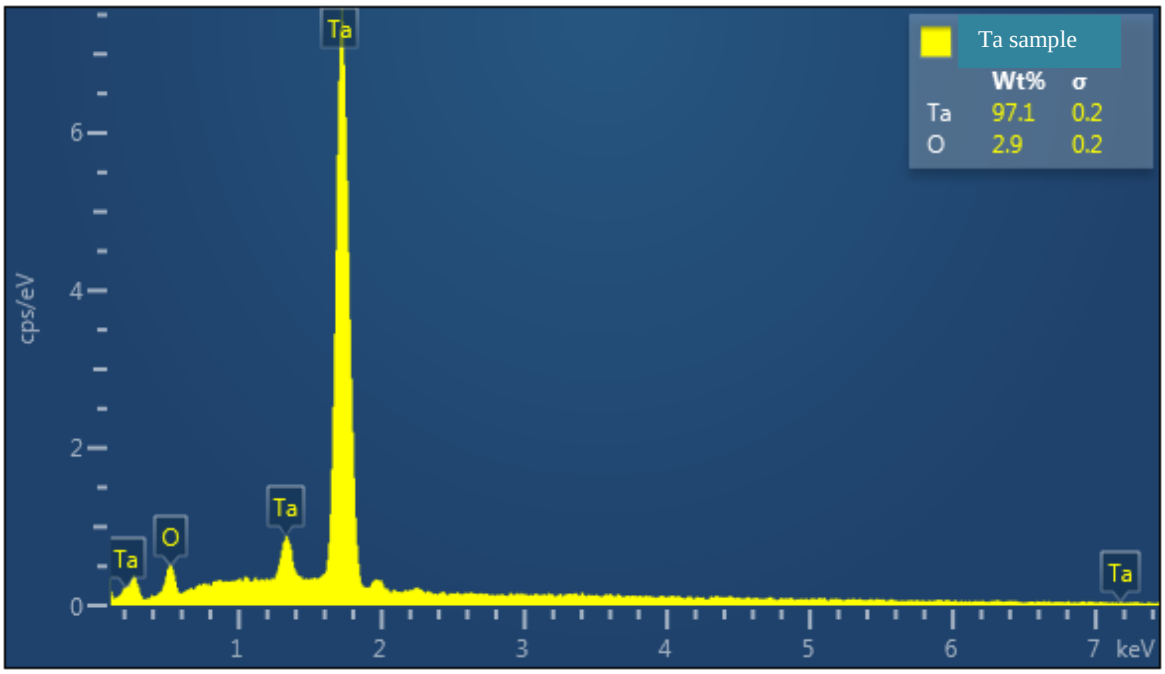

Figure A1 – EDS spectrum of anodized tantalum surface.

ANNEX B – SEM IMAGES OF TANTALUM SURFACES ANODIZED AT DIFFERENT POTENTIALS

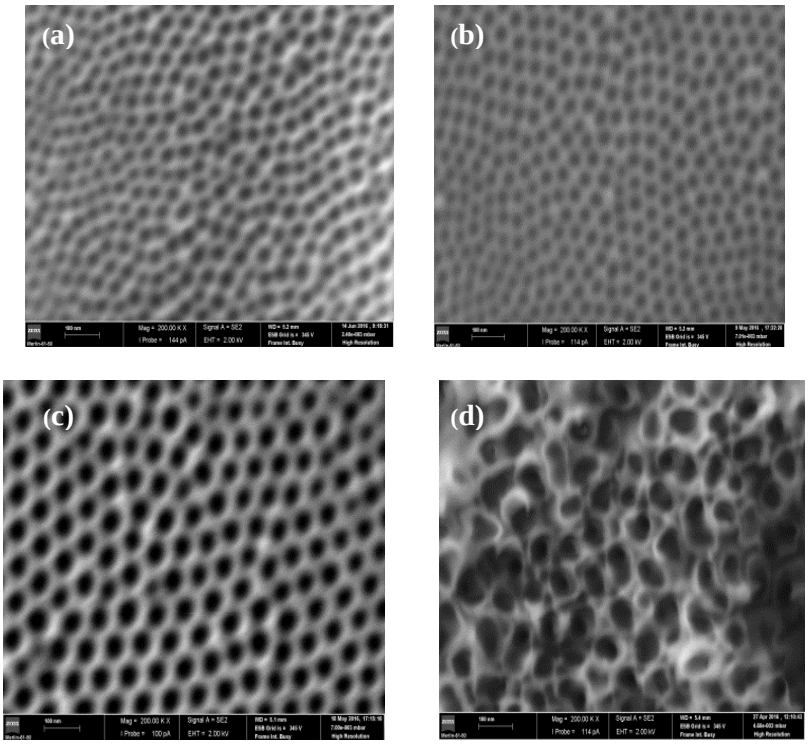

Figure B1. SEM images (200000X magnification) of Ta surfaces treated at different conditions (a) Polished and anodized at 15 V (b) Polished, etched and anodized at 15 V (c) Polished, etched and anodized at 25 V (d) Polished, etched and anodized at 50 V.